TRAINING EFFECT ON THE TWO-WAY SHAPE MEMORY BEHAVIOR OF NITIHF HIGH TEMPERATURE SHAPE MEMORY ALLOY

ŞEKİL HAFIZA EĞİTİMİNİN NİTİHF YÜKSEK SICAKLIKLI ŞEKİL HAFIZALI ALAŞIMIN İKİ YÖNLÜ ŞEKİL HAFIZA DAVRANIŞI ÜZERİNDEKİ ETKİSİ

HÜSEYİN CEMAL TAŞTAN

PROF. DR. BENAT KOÇKAR

Supervisor

Submitted to Graduate School of Science and Engineering of Hacettepe University

as a Partial Fulfillment to the Requirements

for the Award of the Degree of Master of Sciences

in Mechanical Engineering

2022

ABSTRACT

TRAINING EFFECT ON THE TWO-WAY SHAPE MEMORY BEHAVIOR OF NITIHF HIGH TEMPERATURE SHAPE MEMORY ALLOY

Hüseyin Cemal TAŞTAN

Master of Sciences, Department of Mechanical Engineering

Supervisor: Prof. Dr. Benat KOÇKAR

June 2022, 76 pages

Shape Memory Alloys (SMAs) with transformation temperatures (TTs) higher than 100°C are generally utilized for high-temperature actuation applications in the aerospace industry and are called as High-Temperature Shape Memory Alloys (HTSMAs). SMAs have the ability to remember their deformed and undeformed shapes via heating and cooling against applied load. While the One-Way Shape Memory Effect (OWSME) refers to remembering the undeformed shape of the material after deformation via heating, Two-

Way Shape Memory Effect (TWSME) is the phenomenon corresponding to the remembering of both the deformed and undeformed shapes via heating and cooling, respectively. To realize the TWSME in the SMAs, specific thermo-mechanical training procedures should be conducted. This training procedure either includes loading and unloading cycles at a specific temperature (i.e., superelastic training) or heating-cooling cycles under applied constant stress (i.e., isobaric training).

In this study, TWMSE of Ni50Ti25Hf25 (at%) was maintained via following the isobaric training cycles. Ni50Ti25Hf25 (at%) HTSMA was produced using high purity Ni, Ti, and Hf elements via vacuum induction melting. Then it was placed in a mild steel can for applying hot extrusion at 900°C with a 4:1 area reduction, and the material was received as in the extruded condition. While one part of the batch was solution heat-treated (i.e., solutioning, homogenized) at 1050°C for 2 hours, the other part was kept in as extruded condition. Both solutionized and extruded samples were cut into dog bone-shaped tensile test samples using Wire Electron Discharge Machine (WEDM) and mechanically ground to remove the WEDM and oxidation residues from the surfaces.

Both homogenized and extruded samples were first thermally cycled without applying load to understand the effect of extrusion and homogenization heat treatment on the TWSM behavior of the alloy. The degradation of TWSME with the annihilation of dislocations, which were induced by extrusion, was observed. Then, the extruded and the homogenized samples were isobarically trained under 300 MPa constant stress to achieve TWSME and to maintain the stability of this effect for long thermal cycles. After 100 training cycles, the samples were thermally cycled without applying load to characterize TWSME. Finally, TWSM strain (ε_{TWSM}) values were determined from the strain vs. temperatures curves obtained from the stress-free thermal cycles, and it was found that ε_{TWSM} values of the extruded sample decreased from 0.4% down to 0.35% and ε_{TWSM} values of the homogenized sample increased from 0.18% to 0.35%. All the rationale behind these observations was discussed in this study.

Keywords: High Temperature Shape Memory Alloys, Two-way Shape Memory Effect, Superelastic Training, Actuation Strain

ÖZET

ŞEKİL HAFIZA EĞİTİMİNİN NİTİHF YÜKSEK SICAKLIKLI ŞEKİL HAFIZALI ALAŞIMIN İKİ YÖNLÜ ŞEKİL HAFIZA DAVRANIŞI ÜZERİNDEKİ ETKİSİ

Hüseyin Cemal TAŞTAN

Yüksek Lisans, Makina Mühendisliği Bölümü

Tez Danışmanı: Prof. Dr. Benat KOÇKAR

Haziran 2022, 76 sayfa

100°C'den daha yüksek dönüşüm sıcaklıklarına sahip Şekil Hafızalı Alaşımlar (ŞHA'lar) genellikle havacılık endüstrisindeki yüksek sıcaklık eyleyici uygulamaları için kullanılır ve Yüksek Sıcaklık Şekil Hafızalı Alaşımlar (YSŞHA) olarak adlandırılır. ŞHA'lar, uygulanan yüke karşı ısıtma ve soğutma yoluyla deforme olmuş ve deforme olmamış şekillerini hatırlama yeteneğine sahiptir. Tek Yönlü Şekil Hafıza Etkisi (TYŞHE), deformasyon sonrası malzemenin deforme olmamış şeklinin ısıtma yoluyla hatırlanmasını ifade ederken, İki Yönlü Şekil Hafıza Etkisi (İYŞHE), hem deforme olmuş hem de deforme olmamış şekillerin sırasıyla ısıtma ve soğutma yoluyla hatırlamasına denir. İYŞHE'yi ŞHA'larda gerçekleştirmek için özel termo-mekanik eğitim prosedürleri uygulanmalıdır. Bu eğitim prosedürü, belirli bir sıcaklıkta yükleme ve boşaltma çevrimlerini (yani süper elastik eğitim) veya uygulanan sabit gerilim altında ısıtma-soğutma çevrimlerini (yani izobarik eğitim) içerir.

Bu çalışmada, Ni50Ti25Hf25'in İYŞHE'si aşağıda anlatılacak olan izobarik eğitim döngüleri aracılığıyla elde edilmiştir. Ni50Ti25Hf25 YSŞHA, vakum indüksiyon eritme yoluyla yüksek saflıkta Ni, Ti ve Hf elementleri kullanılarak üretilmiştir. Daha sonra 4:1 alan küçültme ile 900°C'de sıcak ekstrüzyon uygulamak için yumuşak çelik bir kutuya yerleştirilmiş ve ekstrüde edilmiş malzeme bu halde temin edilmiştir. Temin edilen parçanın bir kısmı 2 saat süreyle 1050°C'de solüsyonla ısıl işleme tabi tutulurken (yani homojenize edilirken), diğer kısım ekstrüde edilmiş durumda tutulmuştur. Hem homojenize edilmiş numune hem de ekstrüde edilmiş numuneler, Wire Electron Discharge Makinesi (WEDM) kullanılarak köpek kemiği şeklindeki çekme testi numuneleri halinde kesilmiş ve yüzeylerden WEDM ve oksidasyon kalıntılarını temizlemek için mekanik olarak zımparalanmıştır.

Hem homojenize edilmiş hem de ekstrüde edilmiş numuneler, ekstrüzyon ve homojenizasyon ısıl işleminin alaşımın iki yönlü şekil hafıza davranışı üzerindeki etkisini anlamak için ilk olarak yük uygulanmadan termal olarak döngüye tabi tutulmuştur. İYŞHE'nin ekstrüzyon sebebi ile oluşan dislokasyonların yok olmasıyla kaybolması gözlemlenmiştir. Daha sonra, ekstrüde edilmiş ve homojenize edilmiş numuneler, İYŞHE'yi elde etmek ve uzun termal döngüler için bu etkinin stabilitesini korumak için 300 MPa sabit gerilim altında izobarik olarak eğitilmiştir. 100 eğitim döngüsünden sonra, numuneler İYŞHE'yi karakterize etmek için yük uygulanmadan termal olarak döngüye alınmıştır. Son olarak, gerilimsiz termal döngülerden elde edilen gerinim-sıcaklık eğrilerinden İYŞH gerinim değerleri belirlenmiş ve ekstrüde edilen numunenin İYŞHE gerinim değerlerinin %0,4'ten %0,35'e düştüğü ve homojenize edilen numunenin İYŞHE gerinim değerlerinin %0,18'den %0,35'e yükseldiği tespit edilmiştir. Bahsedilen gözlemlerin ve çıkarımların arkasındaki sebepler bu çalışmada değerlendirilmiştir.

Anahtar Kelimeler: Yüksek Sıcaklık Şekil Hafızalı Alaşımlar, İki Yönlü Şekil Hafıza Etkisi, Süperelastik Eğitim, Eyleyici Gerinimi

ACKNOWLEDGEMENTS

I would like to express my gratitude to my supervisor Prof. Dr. Benat KOÇKAR, for her endless patience and support. Without her guidance throughout the project, it might not be possible to compose the present study. Therefore, I would like to thank her for believing in me.

I wish to extend my special thanks to my friends at the Hacettepe University Mechanic and Microstructure Laboratory, Oğulcan Akgül, Halil Onat Tuğrul, and Erhan Akın, for their support.

I also wish to show my appreciation to Turkish Aerospace Industries (TAI), Inc. and my colleagues, Haldun Halis, Eren Duzcu, and Mustafa Bal, for supporting me during my studies. This study was supported by Turkish Aerospace Industries (TAI) under Grant no. DKTM/2015/10, therefore, I would like to express my sincere gratitude to TAI once more.

Finally, I would like to thank my mother, Nuran Taştan, my father, Selman Taştan, and my sister, Sevde Nur Taştan, for their self-sacrificing devotion to encouraging me. I am deeply indebted to my family for always loving me and backing me up.

Hüseyin Cemal TAŞTAN

June 2022, Ankara

TABLE OF CONTENTS

LIST OF FIGURES

LIST OF TABLES

SYMBOLS AND ABBREVIATIONS

Abbreviations

SE	Superelastic Effect
SME	Shape Memory Effect
OWSME	One-way Shape Memory Effect
TWSME	Two-way Shape Memory Effect
TWSM	Two-way Shape Memory
LPDS	Linear Potentiometric Displacement Sensor
UCT	Upper Cycle Temperature
LCT	Lower Cycle Temperature
A_f	Austenite finish temperature
A_s	Austenite start temperature
M_f	Martensite finish temperature
M_s	Martensite start temperature
Ni	Nickel
Ti	Titanium
Hf	Hafnium
SMA	Shape Memory Alloy
HTSMA	High-Temperature Shape Memory Alloy
ECAE	Equal Channel Angular Extrusion
TT	Transformation Temperature
WEDM	Wire Electron Discharge Machine
FFTS	Functional Fatigue Test Setup

Symbols

ε_{irr}	Irrecoverable strain
ε_{TWSM}	TWSM strain
ε_{mar}	Martensite strain
ε_{aus}	Austenite strain
TT	Transformation temperature
ΔT	Temperature hysteresis

1. INTRODUCTION

SMAs are promising materials that have the ability to remember their original shapes due to showing reversible martensitic transformations. SMA can recall its undeformed shape above A_f temperature by simply removing applied stress, which is called the Superelastic or Pseusedoelastic Effect (SE). Also, they can recover their original shape after deformation when they are heated above a specific characteristic temperature [1–9]. While this property is known as Shape Memory Effect (SME), it can be divided into two categories such as OWSME and TWSME [7, 10–14]. As explained in later sections, a resetting force is required for the OWSME, but it is not necessary for the TWSME, making the TWSME more favorable, especially for actuation required applications. It should be noted that TWSME can be attained by applying training procedures, which will be discussed in the later chapter.

SMAs can be used as solid-state actuators because of their capability to work against load. Compared to conventional actuators such as hydraulic, D.C. motor, or pneumatic driven actuators, SMA actuators have some promising features. Easier inspection and maintenance due to reduction in total part count, higher energy density due to light-weight, and smooth motion due to frictionless and quiet design could be regarded as the most promising features of SMA actuators [2, 10, 15–20]. Also, the utilization of SMAs is simpler than that of the solenoid or piezoelectric actuators with higher recoverable strain levels, i.e., higher energy density [21].

Owing to their favorable shape memory properties, such as relatively better dimensional stability, ductility, and workability, among various SMAs, NiTi binary SMAs are the most known and commercially employed SMAs, especially for medical and engineering applications. However, NiTi binary SMAs cannot be utilized effectively, for instance, in the aerospace, automotive, or energy sector, because their TTs are below 100°C. The TTs below 100°C might cause unintentional actuation in high-temperature actuation required cases. Adding a ternary element in binary NiTi SMAs or altering their stoichiometry are suggested as efficient methods to increase TTs. To tackle the low TT drawback of NiTi binary (i.e., to increase the TTs to above 100°C), alloying with Pd, Pt, Au, Hf, and Zr is

proposed as one of the convenient methods in the literature, which makes NiTi SMAs as HTSMAs [14, 20, 22]. While NiTi SMAs have TTs below 100°C, by adding the third element in the alloy, the TTs of HTSMAs can be increased up to 400°C and higher. Among the elements mentioned above, Pd, Pt, and Au precious elements were suggested as the most competent in increasing the TTs. Additionally, it is stated that especially NiTiPd has considerable potential because of showing narrow thermal hysteresis (ΔT) and acceptable strain recovery [10, 15].

Although the Pd, Pt, and Au additions can increase the TTs effectively, because of the high cost of these precious materials, Hf and Zr have been taking considerable attention recently [15]. However, since it is stated that Hf is more effective in terms of raising the TTs to 400°C than that of Zirconium and NiTiHf HTSMAs have proved themselves for the high strength and temperature applications, and they have attracted higher attention compared to Zirconium [2, 21]. Apart from having a TT above 100°C, NiTiHf HTSMAs could be employed in high temperature and strength applications since shape memory and superelasticity effect can be observed under 500 MPa and higher stress magnitudes [3]. While there are numerous investigations on the SMAs, it is stated that the studies on the shape memory characteristics of the NiTi-based HTSMAs are still insufficient[15]. Although relatively wider ΔT of NiTiHf HTSMAs is known as one of the drawbacks, by doing thermomechanical and microstructural optimizations, NiTiHf HTSMAs could become a promising alternative and can be preferred to be used commercially. In fact, it is suggested that with more than 10-15% Hf content in the NiTi binary, relatively less ΔT and higher TTs could be achieved [2].

As mentioned above, since the number of research on the NiTiHf HTSMAs in the literature is limited and there has been almost no systematical study on the TWSME of NiTiHf alloy with very high Hf content, SMA properties together with the TWSME evolution of Ni50Ti25Hf25 (at%) HTSMA were investigated in this study. Firstly, one of three Ni50Ti25Hf25 (at%) specimens were homogenized at 1050°C for two hours, and the other two specimens remained as extruded to observe the homogenization effect on the TWSME evolution of the alloy. Throughout the study, the homogenized specimen is referred as “H2” and the first and second extruded samples are introduced as “E” and

"EE", respectively. Then, to investigate the effect of shape memory training on the TWSME of Ni50Ti25Hf25 (at%), 100 isobaric training cycles were performed on all three samples because it was proposed in previous studies that 100 training cycles are usually sufficient to obtain a stable TWSME [21]. On the other hand, Ni50Ti25Hf25 (at%) has very high TTs, so there might be a possibility to lose the TWSME with thermal cycling. While the first Extruded sample (E) failed at the 91st training cycle, the other two specimens were able to complete the entire training procedure. Thus, after the training, the effect of training on the Homogenized (H2) and second Extruded (EE) samples was investigated via running 1000 stress-free TWSME cycles.

The aims of the present study are to achieve stable TWSME in very high-temperature Ni50Ti25Hf25 (at%) SMA and to observe the effect of extrusion and homogenization heat treatment on the TWSM behavior of the Ni50Ti25Hf25 (at%) HTSMA. Then, at the end of the 1st 10 stress-free thermal cycles, as will be explained in section 4.2, the degradation of TWSME by the annihilation of extrusion-induced dislocation is shown. In addition, TWSME of the Ni50Ti25Hf25 (at%) HTSMA was achieved and observed for 1000 TWSME cycles by the shape memory training (i.e., training under stress via heating and cooling). Finally, during 1000 TWSME cycles, actuation strain (ε_{act}) values together with the martensite strain (ε_{mar}), austenite strain (ε_{aus}), and ΔT of both extruded and homogenized specimens were obtained and compared. Although some thermomechanical studies have been done on the Ni50Ti25Hf25 (at%) HTSMAs, to the author's best knowledge, the present study has the importance of being the first research in the literature, which shows the training and homogenization effect on the TWSME behavior of Ni50Ti25Hf25 (at%) alloy for 1000 TWSME cycles after isobaric training.

2. THEORY

SMAs are particular materials that can remember their original undeformed shape if heated after deformation. Reversible martensitic phase transformation takes place when SMAs recover their undeformed shape after heating them above a specific characteristic temperature. This phenomenon is called as the SME. In addition, if the material is deformed above a certain temperature, its original shape can be recovered by simply removing the applied load. This property of SMAs is known as the superelastic effect or pseudoelastic effect (SE) [1–9]. SMAs have two stable phases at different temperatures, which are austenite and martensite. While the austenite, i.e., parent phase, is known as the high-temperature phase, martensite exists at low temperatures. Also, there are mainly two structures of the cold phase (martensite): twinned and detwinned martensite. Because of forward (austenite to martensite) and reverse (martensite to austenite) phase transitions, SMAs can show SE and SME. Martensitic transformation is solid to solid first-order phase transformation, which occurs without diffusion. Phase transformations of SMAs can be developed by both temperature and stress applications. For instance, forward transformation takes place due to an increase in the applied stress and/or a decrease in the temperature level [2, 7, 23].

To better understand the parameters of martensitic phase transformation in SMAs, such as TTs, ΔT, actuation (transformation) strain, and irrecoverable strain (ε_{irr}), the standard strain vs. temperature graphic, which can be obtained via running heating-cooling under constant load/stress, is shown in Figure 2.1-1. There are four important TTs, which should be defined, namely martensite start (M_s), martensite finish (M_f), austenite start (A_s), and austenite finish (A_f). While the cooling curve represents the forward transformation starting with M_s and ending with M_f temperatures, the heating curve shows the reverse transformation starting with A_s and ending with A_f temperatures. Moreover, because of the energy dissipation possibly caused by defect generation, which leads to the formation of internal friction along the martensite-austenite phase boundary during transformation, heating and cooling curves do not follow the same path. Instead, there is a ΔT between two curves due to the aforementioned reasons, and dissipated energy is the main reason for observing the thermal or mechanical hysteresis during transformation [1, 2, 7].

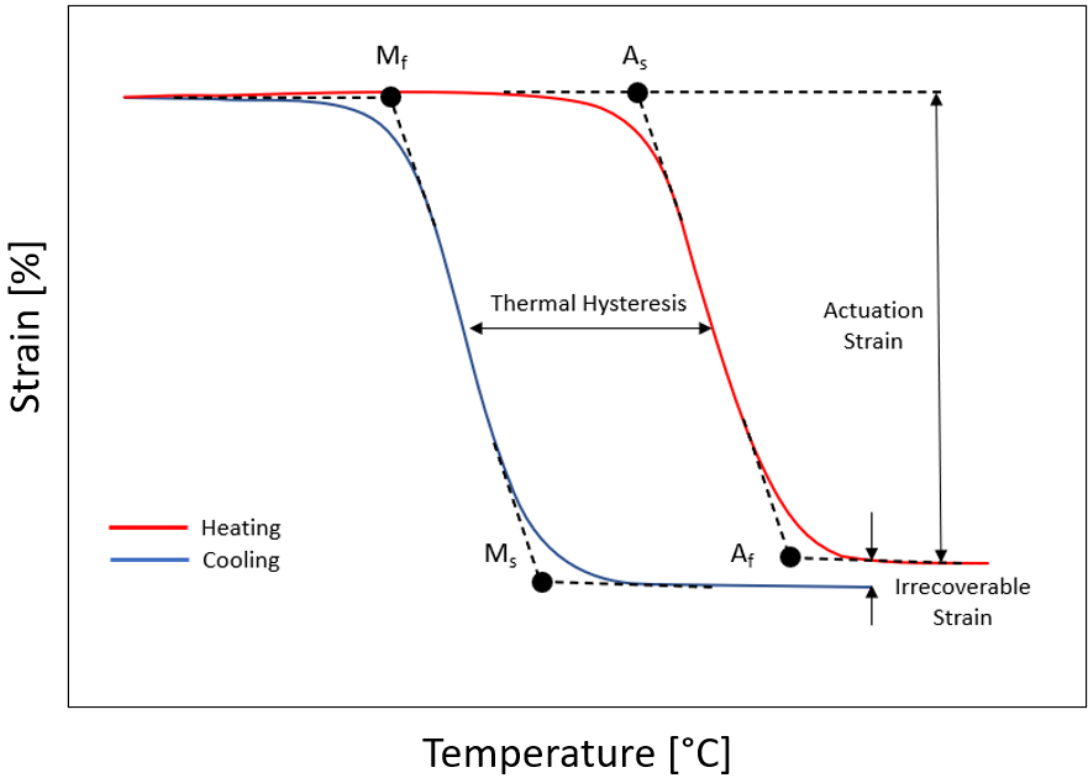

Figure 2.1-1 Strain vs. Temperature Under Constant Load

While thermal hysteresis (ΔT) can be measured between the middle point of the two curves, exact TTs cannot be directly taken as a specific point on curves. Thus, as shown in Figure 2.1-1, tangent lines are drawn using the curves and intersection points of the tangent lines are accepted as the TTs. Other important parameters of SMAs are ε_{irr}, $\varepsilon_{mar,}$ and $\varepsilon_{aus,}$ and the difference between ε_{mar} and ε_{aus}, which is stated as ε_{act}. SMAs cannot always recover the entire strain level; instead, some ε_{irr} may occur due to irreversible plastic deformation during transformation. This plastic strain or ε_{irr} retains in the material as residual strain. Actually, ε_{aus} represents the accumulation of this residual strain, which occurs in each cycle. Take a SMA that can be deformed to 10% strain, for instance. Upon heating, if 9% strain is recovered, the remaining 1% is regarded as irreversible plastic strain and it maintains in the material as residual strain. Although the common reason for ε_{irr} is regarded as dislocation formation during transformation, different suggestions can be found in the literature [1, 2, 10].

2.1. Superelastic Effect (SE)

In Figure 2.1-1, the typical stress vs. strain curve is shown to explain the SE of SMAs. It is known that if stress is applied at a temperature above A_f, i.e., while the material is in the austenite phase (point 1), after elastic deformation of austenite between points 1 and 2, the phase transformation starts to occur at point 2. During loading, from point 2 to point 3, the material transforms from austenite to detwinned martensite and at point 3, transformation is completed. Additional stress increment after point 3 leads to only elastic deformation of the detwinned martensite.

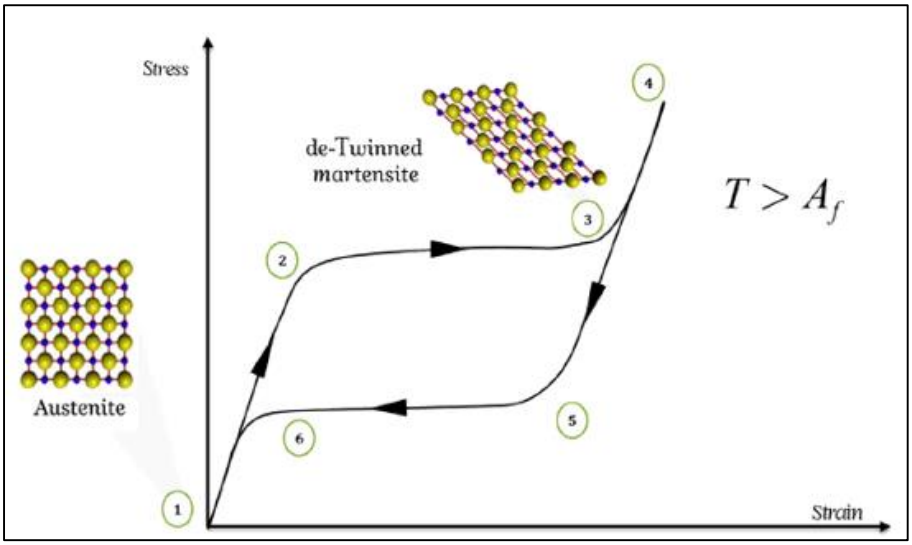

Figure 2.1-1 Stress vs. Strain Curve for The Superelasticity Effect [7]

Upon unloading, starting at point 4, elastic recovery of detwinned martensite takes place and the reverse phase transformation starts. Between points 5 and 6, a large amount of strain is recovered and the material remembers its original shape while transforming to the austenite phase. Therefore, SMAs can remember their original shapes after unloading while deformed above A_f due to the SE. Please note that since the temperature is not a variable for SE, it is assumed constant in the stress vs. strain plot.

2.2. One-Way Shape Memory Effect (OWSME)

To realize the SME, SMAs should be heated after deforming them in their martensite phase, as shown in Figure 2.2-1. Unlike the SE, stress is applied to the material at the

twinned martensite phase and elastic deformation occurs between points 1 and 2. After point 2, the martensite phase starts to reorient its structure from twinned martensite to detwinned martensite. Further increase in the stress level leads to an only elastic strain of detwinned martensite.

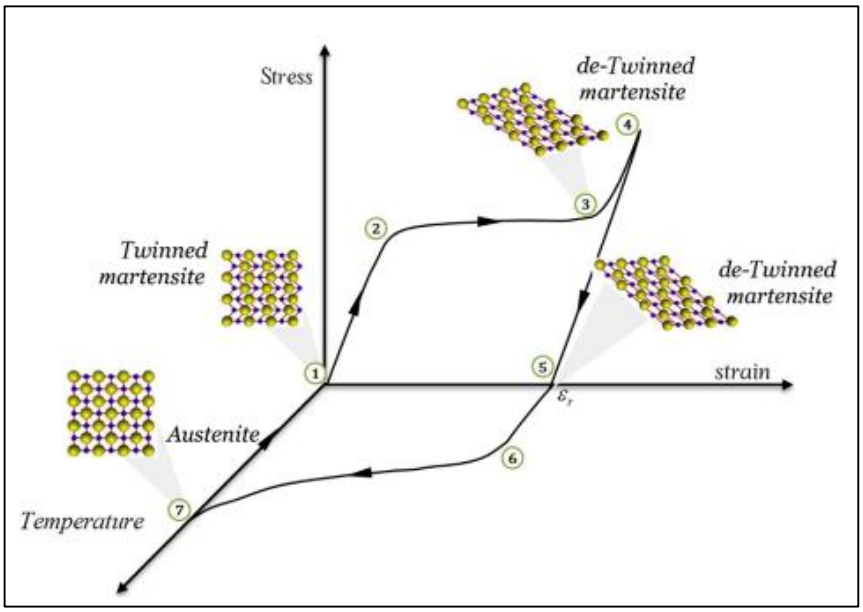

Figure 2.2-1 Stress vs Strain vs Temperature Curve For The Shape Memory Effect [7]

After unloading from point 4 to point 5, the material presents residual strain due to the detwinned martensite structure at point 5. This residual strain can be recovered by heating the material above a characteristic temperature, which is named as A_f. Between points 5 to 7, a macroscopic shape change occurs and the material transforms from detwinned martensite to parent phase austenite by the increase in temperature. Finally, if the material is cooled down to the initial temperature, austenite thermally transforms to twinned martensite at point 7. Please note that a macroscopic shape change can be observed from detwinned martensite to austenite phase transformation (between points 5 and 7). Thus, SMAs can recover their undeformed shape by heating after unloading. The material's ability to remember its original shape upon heating is measured by ε_{act}. However, if partial recovery of the shape change occurs, then ε_{irr} appears and full transformation cannot be achieved. If this is the condition, then the difference between the strain achieved at the martensite state and the strain observed at the austenite state is called as ε_{act}. Former studies indicated that the higher the stress application, the higher the ε_{act} is measured up

to a certain point during temperature and stress cycling. Since the transformation strain is related to dislocation formation, the excessive increase in the plastic strain due to higher stress application may decrease the SME [21, 24]. As shown in Figure 2.2-1, required stress should be applied to reset the material after the shape recovery to obtain SME, which is actually called One-Way Shape Memory (OWSME).

2.3. Two-Way Shape Memory Effect (TWSME)

After specific thermo-mechanical procedures, a reversible SME that does not require triggering with the application of force can be obtained and this is called TWSME. Since this study aims to investigate the TWSME of SMAs, the theory of the TWSME will be revealed in further sections. While the OWSME refers to remembering the original shape of the material after deformation by heating, TWSME means both the deformed and undeformed shapes can be remembered via heating and cooling, respectively. In other words, the TWMSE is related to the ability of the material to remember its low and high-temperature shapes under stress-free conditions. The comparison of both effects is shown in Figure 2.3-1.

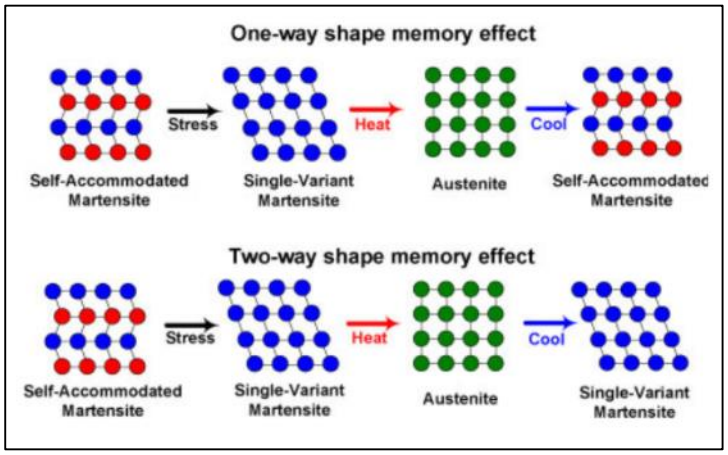

Figure 2.3-1 OWSME and TWSME Mechanisms [2]

However, while the OWSME is an inherent (i.e., natural, intrinsic) characteristic of SMAs, materials should be processed with several thermo-mechanical procedures called training to obtain the TWSME because the TWSME is not an intrinsic feature. To obtain the TWSME, defects and dislocations should be introduced in the alloys that stabilize the corresponding configuration of the martensite twin variants by inducing large strains via following thermo-mechanical training cycles. Thus, just as the material remembers its

original shape when the deformed martensite transforms to austenite, it also remembers its deformed low-temperature shape when the austenite transforms to martensite since the martensite plates remember their configurations due to the training-induced defects, dislocations and the oriented stress/strain field around them. There are several training methods in the literature to obtain TWSME that contains mechanical, thermal and/or thermo-mechanical cycling [7, 10–14].

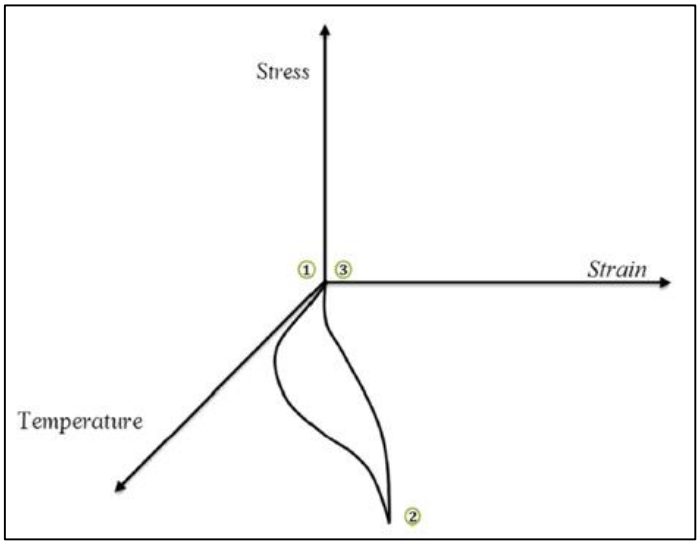

Figure 2.3-2 Strain vs Temperature Curve of TWSME [7]

In the present study, the most common training method, heating and cooling cycling under constant load (i.e., shape memory training) is performed because this method showed satisfactory results in the literature in terms of stability and magnitude of achieved TWSME. Moreover, it is stated that this training method is an effective process and requires a comparatively low level of stress, which causes less plastic strain in the material [10]. Other than that, different training processes are known in the literature, such as stress cycling in austenite (i.e., superelastic training), and deformation cycling in martensite via free or constrained recovery. For the shape memory training, the material is deformed at the austenite state by a constant stress level and cooling-heating cycles are performed, respectively. After several cycles, it is expected that the cold and hot shape of the material can be observed in the absence of stress upon cooling and heating. As mentioned earlier, the main reason for all training procedures is the generation of defects and favorably oriented dislocations/dislocation arrays to create stress/strain fields, which stabilize the configuration of the martensite plates at low temperature [2, 10, 12, 21].

2.3.1. Two-way Shape Memory (TWSM) Mechanism

To better understand the TWSME phenomenon, the mechanism of the effect is explained extensively in this subsection. As aforementioned, SMAs can remember both the high-temperature and low-temperature shapes without applying load and this is called as TWSME. The dislocations, defects, and the stress fields around them generated during training cycles favor the formation and growth of some particular martensite variants at the expense of the others. Thus, during stress-free thermal cycling, these favorable martensite variants grow during cooling and TSWM strain can be observed. Additionally, the dislocations, which are stored during thermo-mechanical training, may pin the martensite boundaries such that martensite plates can still exist although the alloy is heated to A_f temperature. These plates are called as retained martensites, which can act as nucleation sites for the favorable martensite variant formations during cooling the alloy under stress-free conditions. Thus, TWSME can be again obtained due to the formation of these preferential martensite variants.

The other possibility to attain TWSME is the creation of coherent precipitates with aging heat treatment. Coherent precipitates are small enough and stress fields are generated around them due to the misorientation between the atomic arrangement of the precipitates and the matrix. These stress fields again lead to the formation of preferably oriented martensite variants and the formation of retained martensite, which can enable the alloy to show the TWSME without external load. To conclude, as illustrated in Figure 2.3-3, stable dislocation structures, retained martensite formation, and coherent precipitates are suggested as the reasons for internal stress/strain field generations, which enables the TWSME [10, 11, 21].

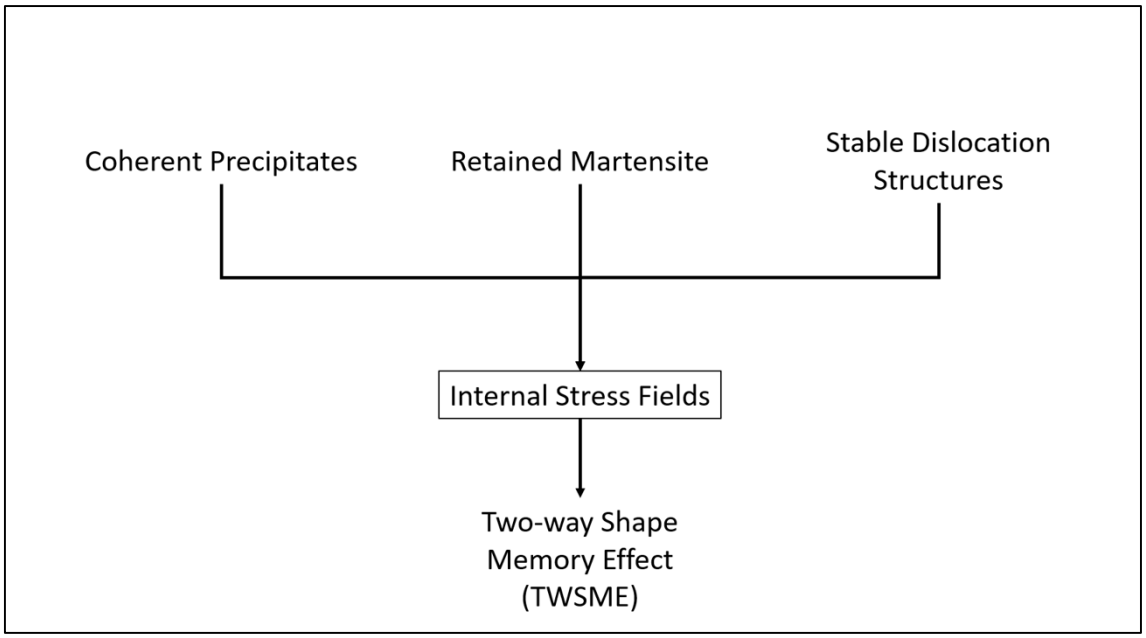

Figure 2.3-3 The possible microstructural features that can be attained with training processes to obtain TWSME

2.3.2. Effect of Dislocations on the TWSME

As is stated, one of the reasons for the oriented stress field in the material that is responsible for the TWSME is stable dislocation structures. It is known that starting from the first cycle of training, the formation of dislocation structures takes place in the material, and during the training process, it continues to develop. Although the TWSME occurs because of dislocations, this does not mean that introduced dislocation in the material always increases the ε_{TWSM}. According to former studies, newly introduced dislocations might stabilize or decrease the ε_{TWSM} of the TWSME, as well, because the effect of dislocations on the TWSME highly depends on the configuration of dislocations [10, 11]. In a study, for instance, it is suggested that dislocation formation created an internal stress or strain field during the first stages of training. After increasing the number of cycles, additional dislocation formation was prevented by the dislocations from the first stages of training. Therefore, the ε_{TWSM} stabilized immediately after the beginning of the training cycles [11].

Also, a similar deduction can be made for stress-free thermal cycles. Trained material shows TWSME strain (i.e., ε_{TWSM} during stress-free thermal cycles) under stress-free

conditions, as explained before. Since stress-induced dislocations are responsible for the internal strain fields and hence the TWSME, ε_{TWSM} during stress-free thermal cycles decreases after training due to internal strain field relaxation and annihilation of dislocations via heating the trained cycles above A_f. After a decrease in ε_{TWSM}, a steady TWSME is observed due to a stable dislocation configuration. It can be concluded that dislocation formation might cause an increase, decrease, and stability in the TWSME. If the accumulation of dislocation during training under constant stress or stress-free thermal cycles happens in the direction of existing oriented strain fields, the TWSME tends to increase. However, if the latter dislocation structures suppress or deteriorate the oriented strain field in the material, the TWSME decreases or stabilizes. Thus, it is suggested in the literature that any method that can direct the dislocation formation in the existing oriented strain fields might increase the TWSM strain and TWSME stability [11]. Moreover, the introduction of dislocation during stress-free thermal cycles is closely linked to the strength of martensite since it is stated that the low strength of martensite allows more accumulation of dislocation, which also means less resistance to stress relaxation. As a summary, high residual strain due to plastic deformation leads to attain excess retained martensite that negatively affects the TWSME, therefore, achieving enough localized plasticity with training is necessary to obtain the stable oriented stress fields around dislocation arrays for observing TWSME via single variant martensite formation [10].

As depicted in Figure 2.3-3, the other reason for the TWSME is retained martensite in the parent phase (i.e., austenite). It is proposed that even above A_f temperature, some martensite variants can stay stable in the austenite by thermomechanical training, which is called retained martensite. Since the retained martensite can act as the site for the formation of preferred martensite variants, the TWSME can be obtained as well. Dislocation formation together with the oriented stress fields around them and retained martensite act as the sites for the corresponding martensite plate (MP) formations during cooling. In other words, repeated mechanical loading or thermal cycles under stress-induced defects, dislocations, and retained martensite. These stabilize some configurations of MP. These plates disappear while heating, but the dislocations and defects still exist. Thus, the same MPs propagate for the internal stress accommodation during the next cooling. The preferred martensite variant formations cause a

macroscopical shape change. Therefore, TWSME still exists while the dislocations do not annihilate.

However, by some heat treatments such as annealing or homogenizing, it is regarded that dislocations are annealed out, which is called annihilation of dislocations. Since one of the main reasons for achieving TWSME is the dislocation accumulation, the annihilation of dislocation decreases the TWSME as well as residual stress fields in the material. As a summary, it is suggested that homogenization after the deformation processes annihilates the deformation-induced dislocations, resulting in a decrease in the ε_{TWSM} during TWSME cycles [24].

2.3.3. Temperature Hysteresis (ΔT)

As shown in Figure 2.1-1, ΔT occurs between heating and cooling curves during temperature and stress cycling. It is suggested that this ΔT, which is called dissipated or stored elastic energy, is related to geometric compatibility between austenite and martensite. To overcome the elastic stored energy, larger stress should be applied or higher temperatures should be achieved for phase transformation during stress and temperature cycling, respectively, which leads to the formation of ΔT. Having such energy dissipation is an undesirable feature of SMAs for actuator applications since more energy to overcome the friction at the martensite-austenite boundary should be supplied for work production. The literature proposes that increasing the geometric compatibility of austenite and martensite decreases the energy dissipation by ΔT. This phenomenon is also explained by stretch tensor. According to the former studies, the middle eigenvalue of stretch tensor measures geometric compatibility. A closer eigenvalue to one indicates more compatibility between hot and cold shape phases. In other words, as shown in Figure 2.3-4, the closer the lambda is to one (i.e., $\lambda=1$), the more compatible the austenite and martensite boundary, leading to more negligible ΔT during phase transformations. Transformation stretch tensor that is shown in Eqn. 1 is a measure that describes the orientation and lattice relationship between the martensite and austenite during martensitic transformation [2, 10, 25].

$$U_1 = \begin{bmatrix} \beta & 0 & 0 \\ 0 & \frac{\alpha+\gamma}{2} & \frac{\alpha-\gamma}{2} \\ 0 & \frac{\alpha-\gamma}{2} & \frac{\alpha+\gamma}{2} \end{bmatrix} \quad \text{(Eqn. 1)}$$

where;

$U_{1:}$ Transformation Stretch Tensor

β: b/a_0

α: a/a_0

γ: c/a_0

a_0: Lattice Parameter of the Austenite

a, b, c: Lattice Parameter of the Martensite

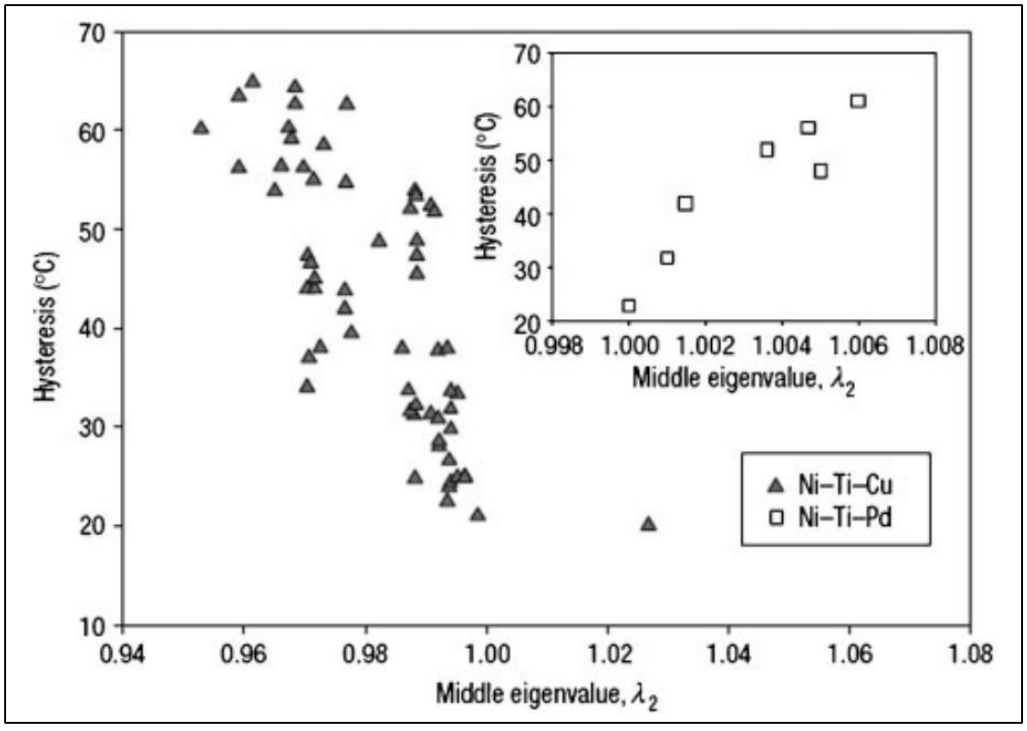

Figure 2.3-4 ΔT vs. Middle Eigen Value of Stretch Tensor in the Ni-Ti-Cu and Ni-Ti-Pd [2]

Low energy dislocation formation is suggested as another reason for ΔT since dissipated work (i.e., ΔT) generally goes into dislocation creation [25]. As is stated in sections 4.3, 4.5, and 4.6, the reason behind observing higher ΔT in the as-deformed sample could be

the geometric incompatibility of austenite and martensite because of deformation-induced existing dislocations.

2.3.4. TWSME of NiTiHf and NiTi-Based HTSMAs

Although the TWSME is a remarkable feature of SMAs because of the elimination of rebiasing force required, the TWSM strain (ε_{TWSM}) is much lower than that of the actuation strain that can be obtained from the OWSME, especially for the NiTiHf HTSMAs [21]. In the literature, a mere 0.25% ε_{TWSM} was calculated for the Ni49Ti36Hf15 (at%) and this value increased to only 0.88% after 7.1% of bending strain at room temperature was applied during training. However, after 10 stress-free thermal cycles, 50% of the ε_{TWSM} was lost due to the degradation in the TWSME [2, 10, 11]. One of the important parameters of HTSMAs is the TWSME efficiency, which is represented by the efficiency factor in the literature. While the ε_{TWSM} of the first TWSME cycle divided by the ε_{act} of the last training cycles yields an efficiency factor, the difference between the ε_{TWSM} of the first and last TWSME cycles divided by the ε_{TWSM} of the first TWSME cycles gives the degradation ratio [10].

There are different ε_{TWSM}, efficiency factor, and degradation ratios reported in the literature. While the first NiTiHf study revealed 1.5% ε_{TWSM} in the ECAEd sample [24]. On the other hand, a much higher ε_{TWSM} was addressed for NiTi binary, which was trained under 80 MPa constant load, 3.06% in the first TWSME cycle. While the efficiency factor was calculated as 0.83 (i.e., ε_{TWSM} was 83% of the last training cycle), since ε_{TWSM} at the 10^{th} cycle was measured 2.75%, TWSM degradation was calculated as 0.1, which means 10% of TWSME degraded at the 10^{th} TWSME cycle. Moreover, isobaric training under 80 MPa was conducted on the NiTiPd HTSMA, and after the training, 2.12% ε_{TWSM} was measured at the 1^{st} TWSME cycle. Also, the efficiency factor and ε_{TWSM} degradation were calculated for the NiTiPd as 0.88 and 0.06, respectively [10]. Another study was conducted on precipitation-hardened Ni-rich NiTiHf torque tubes by training under 500 MPa step-wise constant load for 100 cycles and 3% ε_{TWSM} was found in Ni-rich NiTiHf [26].

Similarly, Ni50.3Ti29.7Hf20 (at%) thin-walled HTSMA tubes showed approximately 3.5% ε_{act} at the 600th isobaric training under 200 MPa stress level with a 0.85 efficiency factor and ε_{TWSM} was determined as 2.95% under stress-free condition[14]. Although there are some studies on the TWSME and ε_{TWSM} of NiTi-based HTSMAs, to the authors' best knowledge, there has not been any report in the literature on the ε_{TWSM} of Ni50Ti25Hf25 (at%) HTSMA that was trained under constant load. It should be mentioned that Ni50Ti25Hf25 (at%) HTSMA is a very high-temperature SMA that shows 500°C austenite finish temperature.

3. EXPERIMENTAL PROCEDURES

3.1. As Received Material

In this study, 50Ni25Ti25Hf (at %) HTSMA was received in the form of extruded rods, and one of them was cut into three sections to conduct the experiments, which are defined in Figure 3.1-1 in detail. Nickel, Titanium, and Hafnium high purity materials were melted by using the vacuum induction melting technique. The chamber of the vacuum induction melting machine was purged several times with argon and then vacuumed to finalize the casting process. After casting, the material was wrapped with a mild steel can to reduce friction between the material surface and extrusion die surfaces. Afterward, at a high temperature of 900°C, wrapped material was hot extruded with an area reduction of 4:1. Before shipping the materials, a turning process was conducted to detach the mild steel can from the material. Therefore, extruded 50Ni25Ti25Hf (at %) HTSMA rods were received without the mild steel can, as shown in Figure 3.1-2. Throughout the below-mentioned experiments, while two samples were kept in as-extruded condition, homogenizing heat treatment was applied later to the remaining sample.

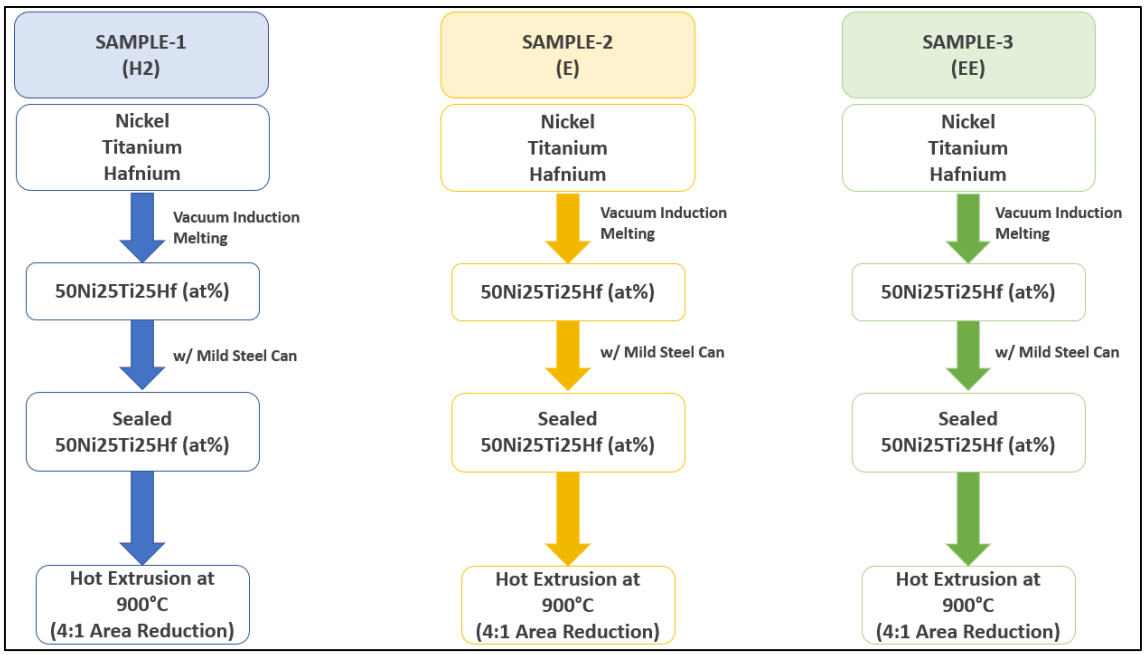

Figure 3.1-1 Processing Route of the 50Ni25Ti25Hf (at %) alloy

Figure 3.1-2 As Received 50Ni25Ti25Hf (at %) alloy extruded rods [1]

3.2. Sample Preparation

To conduct thermo-mechanical experiments on three 50Ni25Ti25Hf (at %) test samples, a custom-built functional fatigue test setup (FFTS) was employed. Since the test setup has specific grips to test dog bone shape tensile samples, the hot extruded alloy was cut in dog bone shape by a wire electrical discharge machine (WEDM). The schematic of the test sample with a flat dog bone shape is given in Figure 3.2-1.

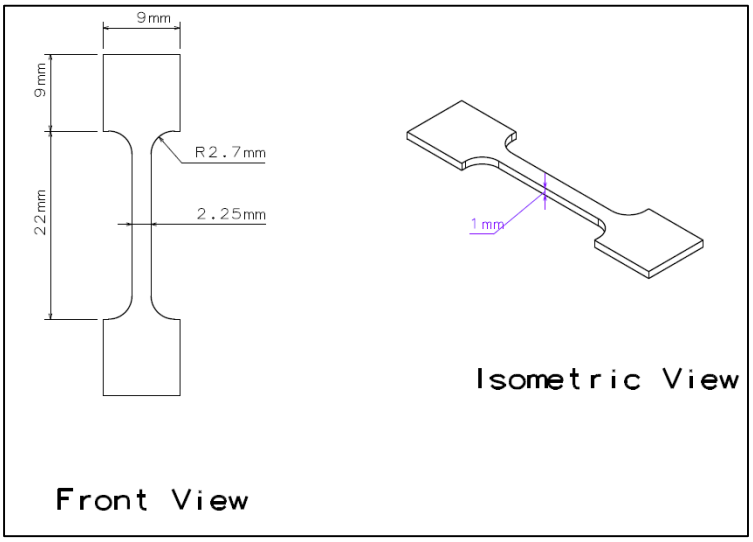

Figure 3.2-1 Flat Dog Bone Shape Test Sample

3.3. Differential Scanning Calorimeter (DSC)

To conduct heating cooling under constant stress experiments at the custom-built functional fatigue test set up, upper cycle temperature (UCT) and lower cycle temperature (LCT), which are set at the beginning of the experiments, should be determined for the 50Ni25Ti25Hf (at %) test samples. Setting the most appropriate UCT and LCT temperatures is extremely important since the samples should fully transform to austenite and martensite by heating and cooling the samples to UCT and LCT, respectively. By obtaining TTs via Differential Scanning Calorimeter (DSC) technique, it became possible to decide the parameters of thermo-mechanical experiments. DSC is regarded as an essential technique to examine the shape memory properties of SMAs, such as TTs, transformation enthalpies, and ΔT during transformation. By supplying heat to the material, exothermic or endothermic reactions can be seen as a function of time and temperature [27, 28]. Thus, TTs, transformation enthalpies, and ΔT can be determined.

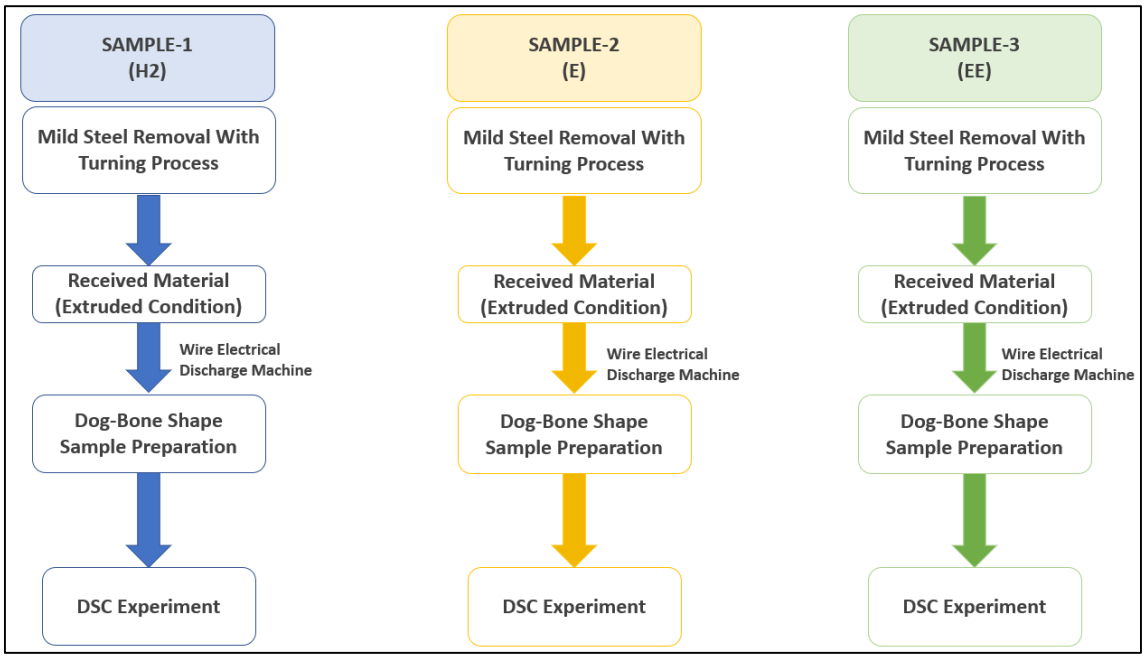

Figure 3.3-1 Experiment Sequence, including DSC experiments

3.4. Surface Preparation

The surfaces of the samples were polished to remove the WEDM residue and oxidation layer that was observed after homogenization heat treatment. As explained in the

following sections, the temperature of the samples was measured using a laser infrared pyrometer; thus, the emissivity value of the sample surface should be known to conduct accurate measurements. Therefore, the surfaces of the samples were sprayed with a high temperature-resistant black paint. While the emissivity value of 50Ni25Ti25Hf (at %) HTSMA sample is not known, the emissivity value of the black painted surfaces was taken as 0.95; therefore, it became possible to measure the temperature of the samples during running the tests. For a proper coating of the surface with the aforementioned black paint and accurate temperature measurement, sample surfaces were mechanically ground until a scratch-free surface was obtained. Since medium to fine grinding was sufficient for our purposes, test specimens were mechanically ground with water-lubricated abrasive papers. For successive medium and fine grinding, the grid sizes of abrasive papers should be finer at every stage. Therefore, from coarser to finer, 240, 320, 400, 600, and 800 grid size abrasive papers were utilized for grinding, respectively. Specimens were washed with water during grinding and before the change of the grinding paper to obtain a scratch-free paint surface. Since material removal was performed by grinding, final specimen dimensions were measured and depicted in Figure 3.4-1. While calculating the cross-sectional area of samples for applying the desired stress level, final specimen dimensions were used.

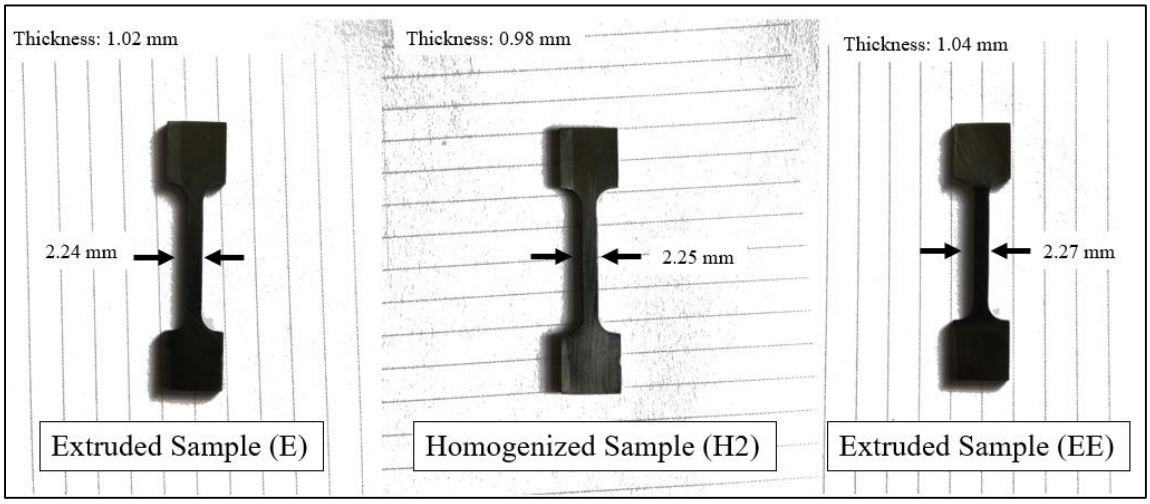

Figure 3.4-1 Final Specimen Dimensions

3.5. Solution Heat Treatment

Solutionizing or homogenization heat treatment (i.e., homogenization, solutionizing heat treatment) was conducted on a 50Ni25Ti25Hf (at %) test sample at 1050°C for two hours using a vertical tube furnace under an argon atmosphere to protect the sample from severe oxidation. The furnace, which was used in this study, is shown in Figure 3.5-1. The additional homogenization step in the experimental sequence is given in Figure 3.5-2.

Figure 3.5-1 Vertical Cylindrical Furnace

The furnace was purged with high purity argon gas and heated to the solutionizing temperature with a 10°C/min heating rate to overcome the overshooting problem during heating. Before beginning to homogenization process at the vertical cylindrical furnace, the test sample was wrapped with a 25.4 μm thick Tantalum Foil to prevent material from further oxidation.

Then the sample was placed in the middle zone of the furnace since the set temperature can be achieved in the middle part, where the control thermocouple is inserted. The sample was held for 2 hours at 1050°C, i.e., homogenized at 1050°C for 2 hours. Then heating was stopped and the furnace cooled down to 300°C. The chamber of the furnace was purged all the time during the heating stage, homogenization stage and the cooling stage as well. Finally, the homogenized sample was taken out from the furnace, which was at 300°C, and the Tantalum Foil was unfolded at room temperature.

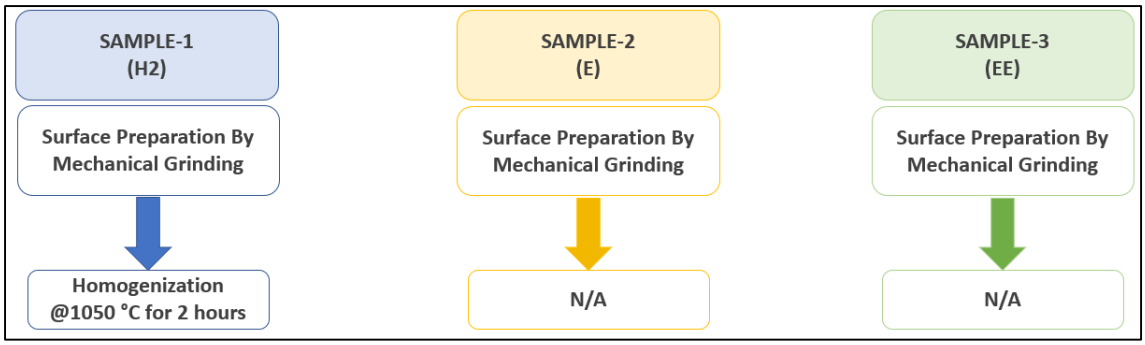

Figure 3.5-2 Experiment Sequence

3.6. Custom-Built Functional Fatigue Test Setup (FFTS)

A custom-built FFTS was utilized for training the HTSMA via heating-cooling under 300MPa constant stress and running the heating-cooling experiments without applying stress to measure the TWSME. The FFTS is schematically shown in Figure 3.6-1. Training cycles and TWSM behaviors of SMAs were examined using the data, which were collected by the data logger system driven with a custom-coded Labview program. The main components of the test setup are listed below and a detailed explanation of the custom-built FFTS is given in the literature [1].

- Mass Holders and Connection Equipment
- Grips
- Dead Weights
- DC Power Supply
- Linear Potentiometric Displacement Sensors (LPDSs)
- Infrared Pyrometer
    - Optris CTlaser LTF-CF1
- Software
    - National Instruments LabView

The desired stress level was obtained throughout the sample cross-section by hanging dead weights to the bottom grip of the sample. The magnitudes of the dead weights were calculated for the desired stress level, which is 300 MPa for this study. Since test

specimens are heated by electrical current and cooled through natural convection, the material of the top and bottom grips of the test setup was selected as hot work tool steels because thermal cycles reach a high temperature of 600°C to 700°C.

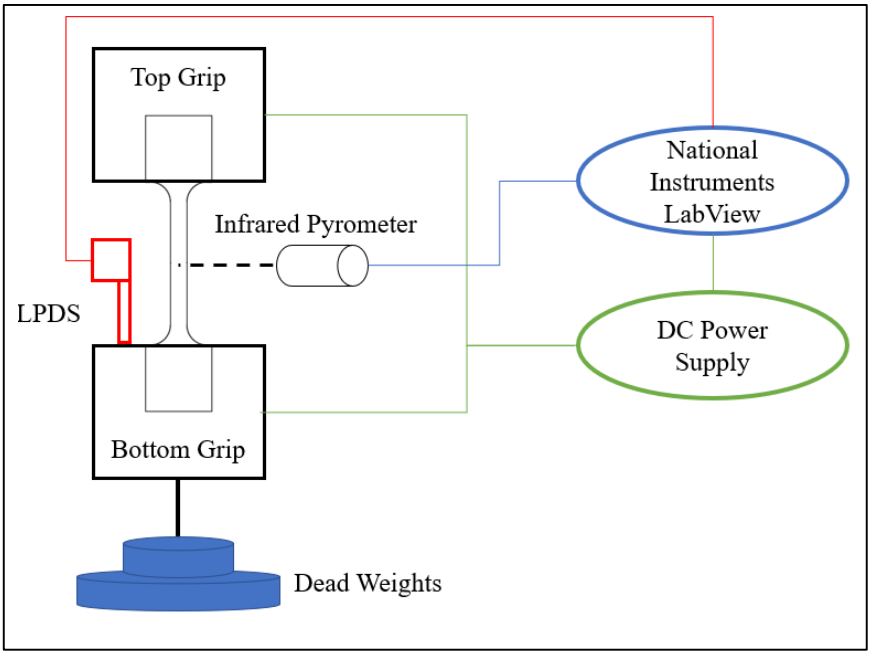

Figure 3.6-1 Custom-Built FFTS

Furthermore, specimens were heated and cooled during training as well as thermally cycling without applying stress experiments in this study, as will be explained in the further sections. A Power Supply was employed as a power source to heat specimens by electrical current and this method of heating is called joule heating in the literature. During the cycles, displacement, temperature and the number of cycles data were collected by the data logger, which was controlled by a LabView program. This program was also used to control the heating-cooling cycle parameters such as UCT, LCT, and heating-cooling rates.

As discussed in further sections, strain vs. temperature graphs of isobaric training and stress-free thermal cycles were plotted to observe shape memory properties and TWSME behavior of the alloy. An LPDS was integrated to measure the displacement of the samples and a laser infrared pyrometer was used to measure the temperature of the sample

surface throughout the cycles. Since thermal emissivity of test specimens is not known, the surfaces of samples were coated with high-temperature black paint, which has 0.95 emissivity value and then the surface temperature of the samples was accurately measured. The black paint is able to stay at the surface without peeling up to around 600°C. When the paint layers were thin enough, the specimen temperature was assumed to be equal to the paint temperature, which was measured by the Infrared Pyrometer.

3.7. Shape Memory Training Cycles

Three Ni50Ti25Hf25 (at%) HTSMA samples have been trained to evaluate their TWSME behavior. The custom-built FFTS was employed for training and TWSM cycling of the samples. To observe TWSME, stress-free thermal cycles were performed, followed by isobaric training cycles. Test samples were placed conveniently between the top and bottom grip of the custom-built test setup.

During training and stress-free thermal cycles, to measure the surface temperature of samples, Optris CTlaser LTF-CF1 infrared thermometer was employed, as mentioned before. Infrared pyrometer is able to measure the surface temperature up to 600°C quite easily and accurately since it is a contactless device, which has a high response to the change in the temperature. While the front surface of the samples was coated with the aforementioned black paint, the surface of the samples, which are in contact with the grips, was not painted because the coating prevents the flow of electrons through the sample; thus, the samples cannot be heated.

Another essential data, which should be collected during experiments, are the displacement values. To calculate the sample strain during cycles, displacement values measured by LVDT were divided by the sample gauge length at each time step. UCT, LCT and heating rate parameters were defined manually in the National Instrument LabView program. LCT, UCT, and heating rate values were set as 200°C, 600°C, and 15°C/s, respectively. A temperature limit was also set as 650°C for the Labview Program since overheating the samples may lead to some undesired changes in the microstructure.

3.7.1. Isobaric Training Cycles

For each Ni50Ti25Hf25 (at%), samples were trained under constant load. First, the sample was placed between electrically conductive grips of the custom-built FFTS. Since the material has higher strength at the Austenite phase, the samples were heated above A_f temperature. To apply the desired stress magnitude to samples, which is 300 MPa, dead weights corresponding to 300MPa were hung at the bottom grip of the test setup while the sample was in the Austenite phase. Since all three samples have different cross-sectional areas, different mass magnitudes were calculated using the equation below and are shown in Table 3.7-1. After loading the samples, the electrical current was cut automatically and waited for the sample to cool down below M_f temperature. Since fast cooling was not required, letting the sample to cool in at open atmosphere was sufficient for the experiment. In other words, the utilization of natural convection is enough to cool the samples below their M_f temperature. Therefore, under constant load, samples were thermally cycled between 600°C UCT and 200°C LCT. To observe and evaluate the TWSM behavior of samples, each of them was trained by conducting 100 isobaric training cycles. The training sequence is given in Figure 3.7-1.

$$m = \frac{\sigma . w . t}{g} \qquad (2)$$

where;

m: Required Mass [kg]
σ: Desired Stress [N/mm^2]
w: Sample Width [mm]
t: Sample Thickness [mm]
g: Gravity [m/s^2]

Table 3.7-1 Mass Magnitude Calculation for Desired Stress Level of 300MPa (units are given above).

Test Sample	Desired Stress	Sample Width	Sample Thickness	Gravity	Required Mass
Homogenized (H2)	300	2,25	0,98	9,81	67,43
As-Extruded (E)	300	2,24	1,02	9,81	69,87
As-Extruded (EE)	300	2,27	1,04	9,81	72,20

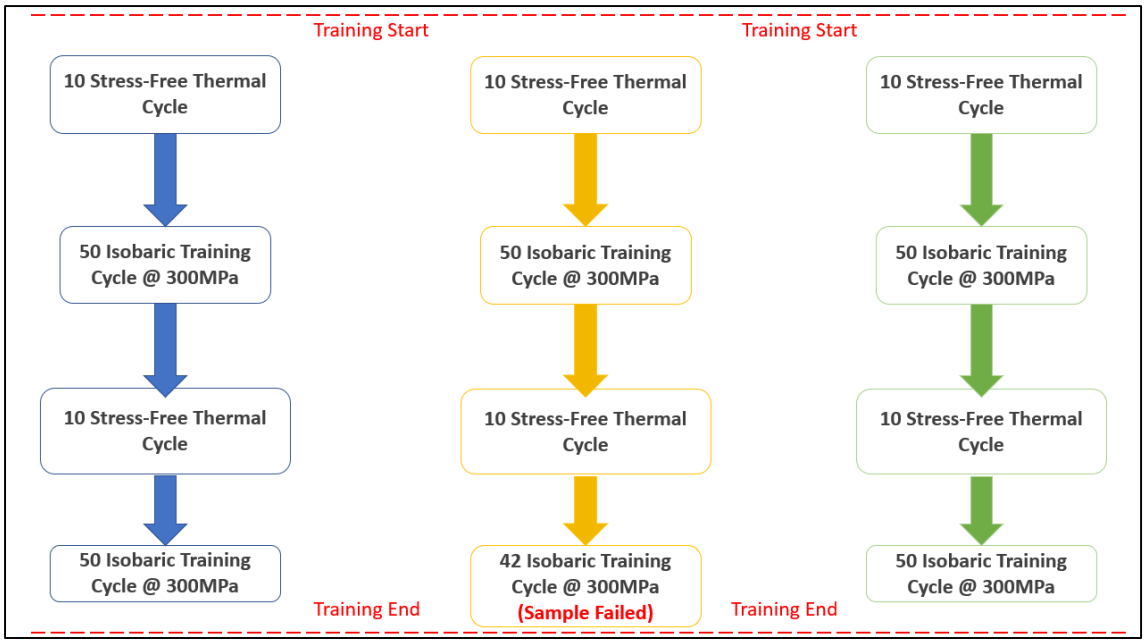

Figure 3.7-1 Training Sequence of the Samples.

3.7.2. Stress-Free Thermal Cycles

TWSM behavior can be observed through running stress-free thermal cycles. Similar to the isobaric training cycles, samples were cycled at stress-free conditions between 600°C UCT and 200°C LCT. The process was identical to isobaric training cycles except for the loading step in isobaric training experiments. After placing samples between test setup grips, samples were heated above A_f temperature and cooled below M_f temperature without hanging dead weights. To calculate the TWSME strain, the hot and cold shape strain difference was measured at every cycle, as suggested in former studies [10]. Before performing any training cycles, all three Ni50Ti25Hf25 (at%) samples were undergone 10 stress-free thermal cycles to investigate the effect of homogenization and extrusion on the TWSME. One homogenized Ni50Ti25Hf25 (at%) sample and two other Ni50Ti25Hf25 (at%) samples in as-extruded conditions were cycled without applying stress for 10 thermal cycles. Moreover, between 100 isobaric training cycles, another 10 stress-free thermal cycles were performed to observe the effect of the first isobaric training. Finally, to compare the TWSM fatigue life of three Ni50Ti25Hf25 (at%) samples, 1000 stress-free thermal cycles were executed. It is worth noting that since the first as-extruded sample failed during isobaric training cycles, it could not be thermally cycled afterward and the TWSM fatigue life of the first as-extruded sample could not be determined. The aforementioned entire experimental steps can be seen in Figure 3.7-2 and Figure 3.7-3 below.

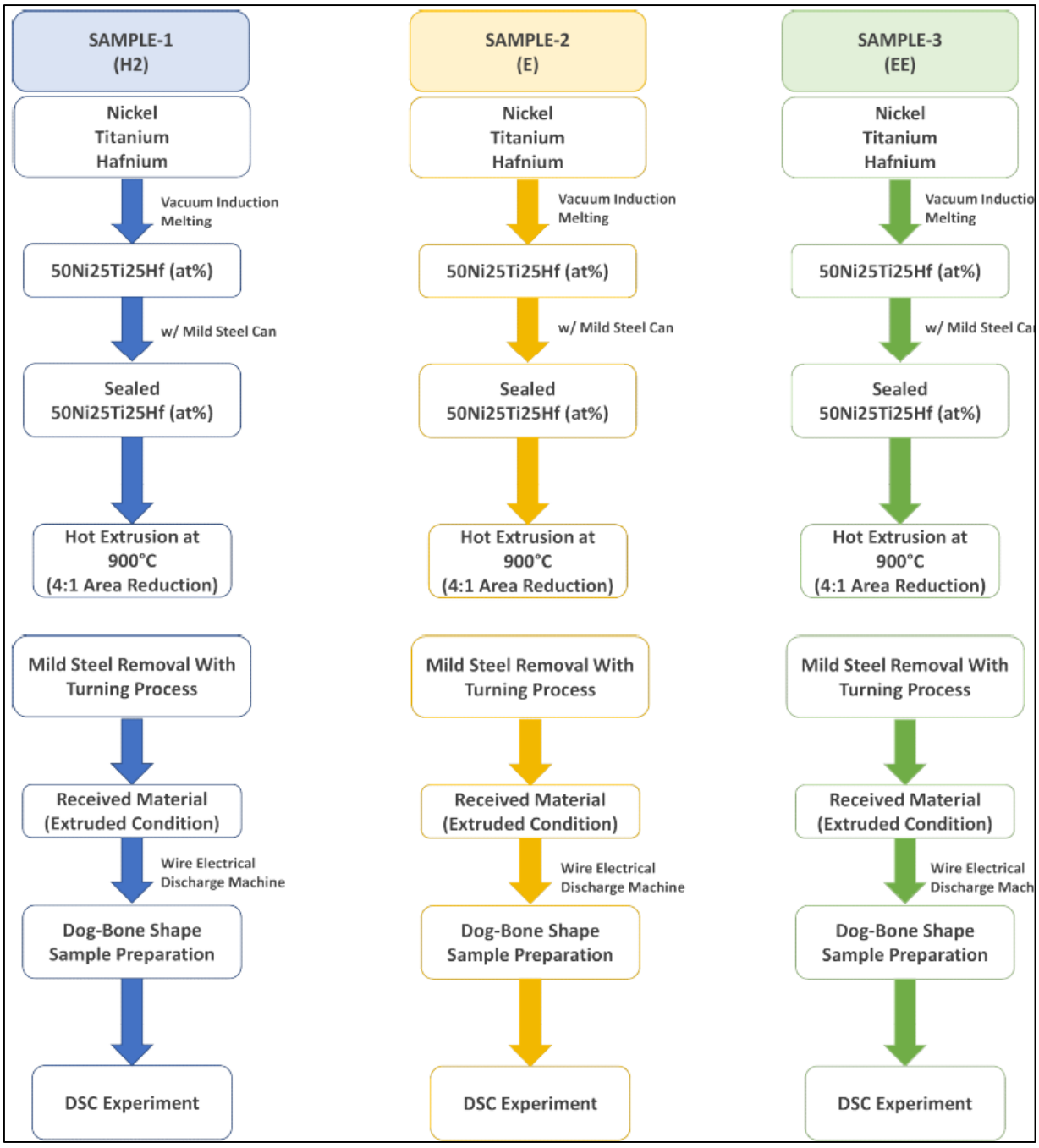

Figure 3.7-2 Entire Experiment Sequence-1

Figure 3.7-3 Entire Experiment Sequence-2 (including 1000 Stress-Free TWSME cycles)

4. EXPERIMENTAL RESULTS

4.1. Differential Scanning Calorimeter (DSC)

In this study, the former results of the DSC experiment, which was conducted on the homogenized 50Ni25Ti25Hf (at %) HTSMA and published before, are used in this study [29]. DSC experiments were conducted between 200°C and 550°C by Perkin Elmer 8000 DSC with a 10°C/min heating and cooling rate. A typical DSC thermogram is illustrated in Figure 4.1-1, and the tangent method to find out the TTs is schematically defined in the figure.

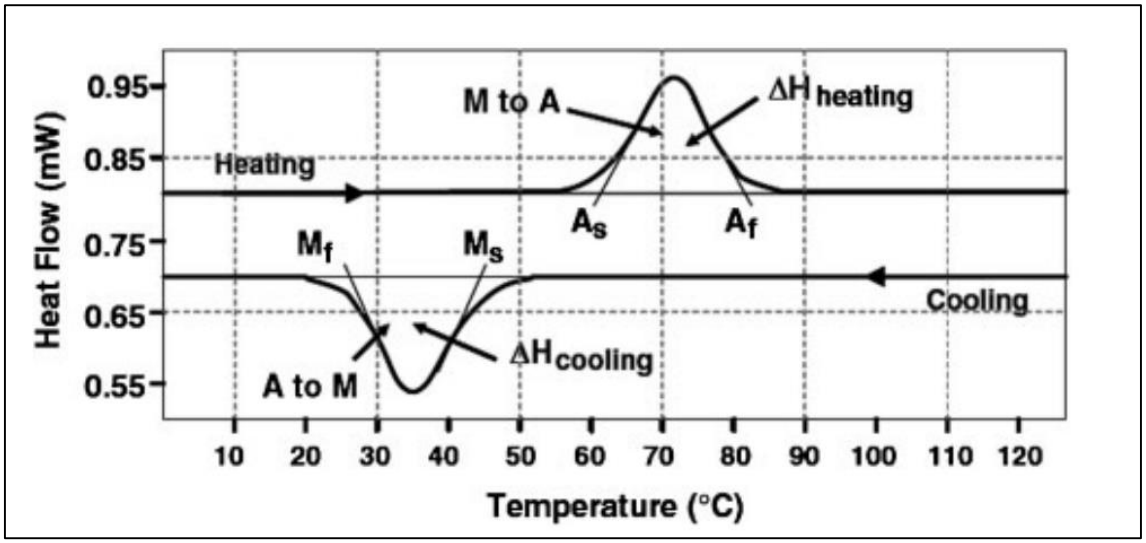

Figure 4.1-1 Typical Normalized Heat Flow vs. Temperature Curves (DSC Thermogram) [2]

The TTs and the ΔT values are given in Table 4.1-1. Since a complete transformation is desired during both stress-free thermal and isobaric training cycles, LCTs and UCTs are defined as 200°C and 600°C, respectively. It is worth noting that the LCTs and UCTs were also selected as 200°C and 600°C for the functional fatigue experiments of homogenized 50Ni25Ti25Hf (at %) sample under 200MPa due to the possible increase in TTs with the applied stress in the literature [30].

Table 4.1-1 The TTs and the ΔT of the Homogenized 50Ni25Ti25Hf (at %) at 1050°C for 2h [30]

	A_s [°C]	A_f [°C]	M_s [°C]	M_f [°C]	ΔT [°C]
Homogenized 50Ni25Ti25Hf (at %) at 1050°C for 2h	399	426	368	294	58

4.2. 1st 10 Stress-Free Thermal Cycles

1st 10 Stress-Free Thermal Cycles were conducted on homogenized and extruded samples to observe the effect of homogenization on the TWSM behavior. While a noticeable ΔT and ε_{TWSM} were observed for the Extruded (E) sample before training, as shown in Figure 4.2-1, the Homogenized (H2) sample did not reveal almost any ΔT or ε_{TWSM} as can be seen in Figure 4.2-2. This could be attributed to the annihilation of extrusion-induced favorably oriented dislocations and/or to the relaxation of extrusion-induced stress fields via solution heat treatment since a similar decrease in the dislocation density was realized after annealing the severe plastically deformed NiTiHf alloy [24]. It has been published many times in the literature for smart metal alloys as well as structural metal alloys that stress relieving and dislocation annihilation can be realized via applying certain heat treatments after deformation processes.

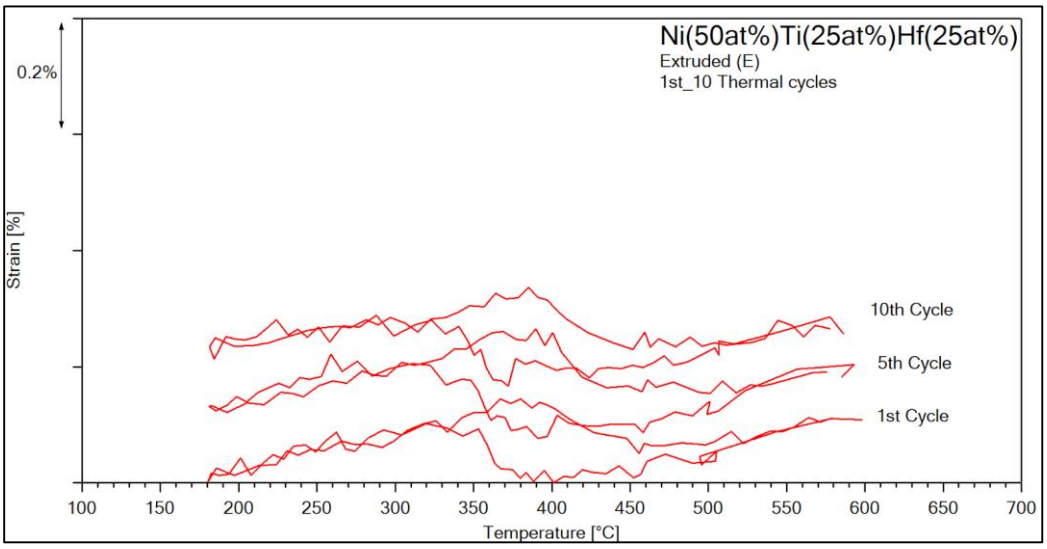

Figure 4.2-1 1st 10 Stress-Free Thermal Cycles of the first Extruded Sample (E)

As explained in the Theory Section, one of the reasons behind the TWSME is the existence of stable dislocation arrays in the microstructure [11]. Since a definite TWSME could not be seen in the Homogenized (H2) sample, it could be speculated that the homogenization deteriorates the favorably oriented dislocation formations and thus, the TWSME was deteriorated as well. Approximately 0.2% ε_{TWSM} was determined at the 10th Thermal cycle of the Extruded sample (E). On the other hand, the homogenized sample did not show any ε_{TWSM} throughout the 10 thermal cycles.

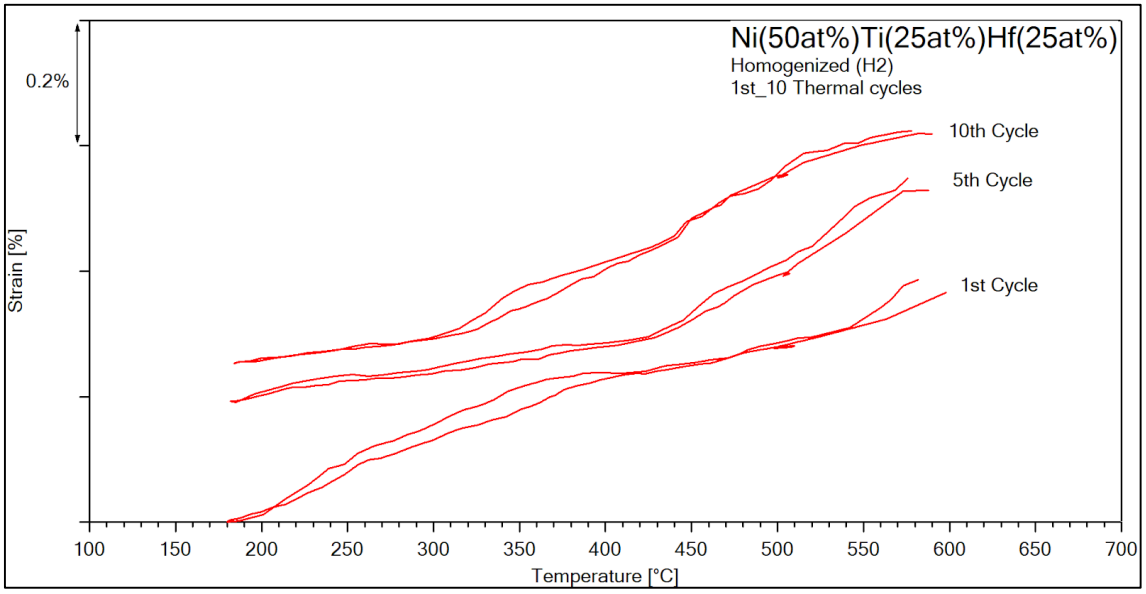

Figure 4.2-2 1st 10 Stress-Free Thermal Cycles of the Homogenized Sample (H2)

Although it can be expected that the first Extruded sample (E) and the second one (EE) would yield a similar result, the second Extruded sample (EE) showed less TWSME than that of the E sample as shown in Figure 4.2-3. This could be related to dislocation annihilation due to uneven cooling of the regions of the extruded alloy after the hot extrusion process. The layers close to the surface of the extruded rod might be cooled faster and the inner layers might be cooled slower. Additionally, the extrusion leads to the formation of microstructural inhomogeneities. It has already been shown in the literature for the Ni50Ti30Hf20 (at%) HTSMA that TTs, $\varepsilon_{act,}$ and ε_{irr} of randomly selected samples from the same extruded billet could vary due to microstructural nonuniformity and deformation variation. Because of the extrusion process, different samples that were cut from distinct parts of the extruded billet may yield different TWSME results, as was observed in the E and EE samples. Therefore, according to the literature, the difference between TWSME behaviors of the first (E) and second Extruded sample (EE) could be regarded as reasonable [29].

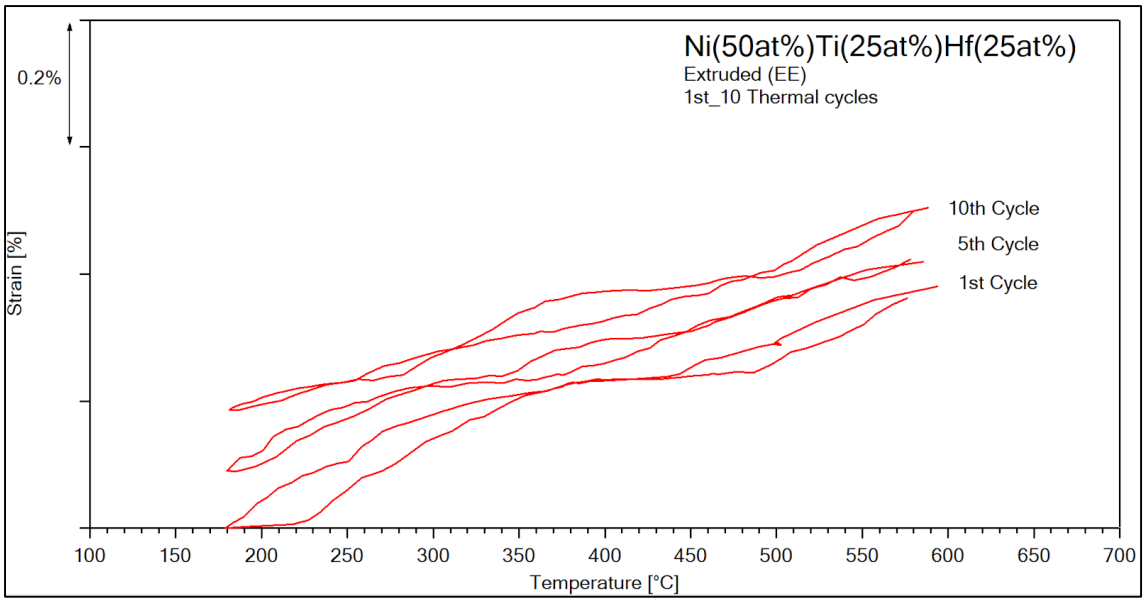

Figure 4.2-3 1st 10 Stress-Free Thermal Cycles of the Second Extruded Sample (EE)

4.3. 1st 50 Isobaric Training Cycles

After observing the effect of homogenization on the TWSM behavior by conducting 10 Stress-Free Thermal Cycles, 50 Isobaric Training Cycles were performed on all three Ni50Ti25Hf25 (at%) HTSMAs under 300 MPa. In Figure 4.3-1(a), all strain vs. temperature curves for 1st 50 Isobaric Training Cycles are shown and strain vs temperature curves obtained every ten cycles were selected and are demonstrated for clear presentation of the training cycles of the Homogenized (H2) sample in Figure 4.3-1(b). It is worth noting that since the resistance of the black paint to very high temperatures, which was used to measure the temperature, is not sufficient for running 100 cycles at once, two 50 Isobaric Training Cycles were conducted in total and the samples were repainted between two training cycle periods. The 1st 50 Isobaric training cycles of the first and second extruded samples are presented in the (a) and (b) parts of Figure 4.3-2 and Figure 4.3-3, respectively.

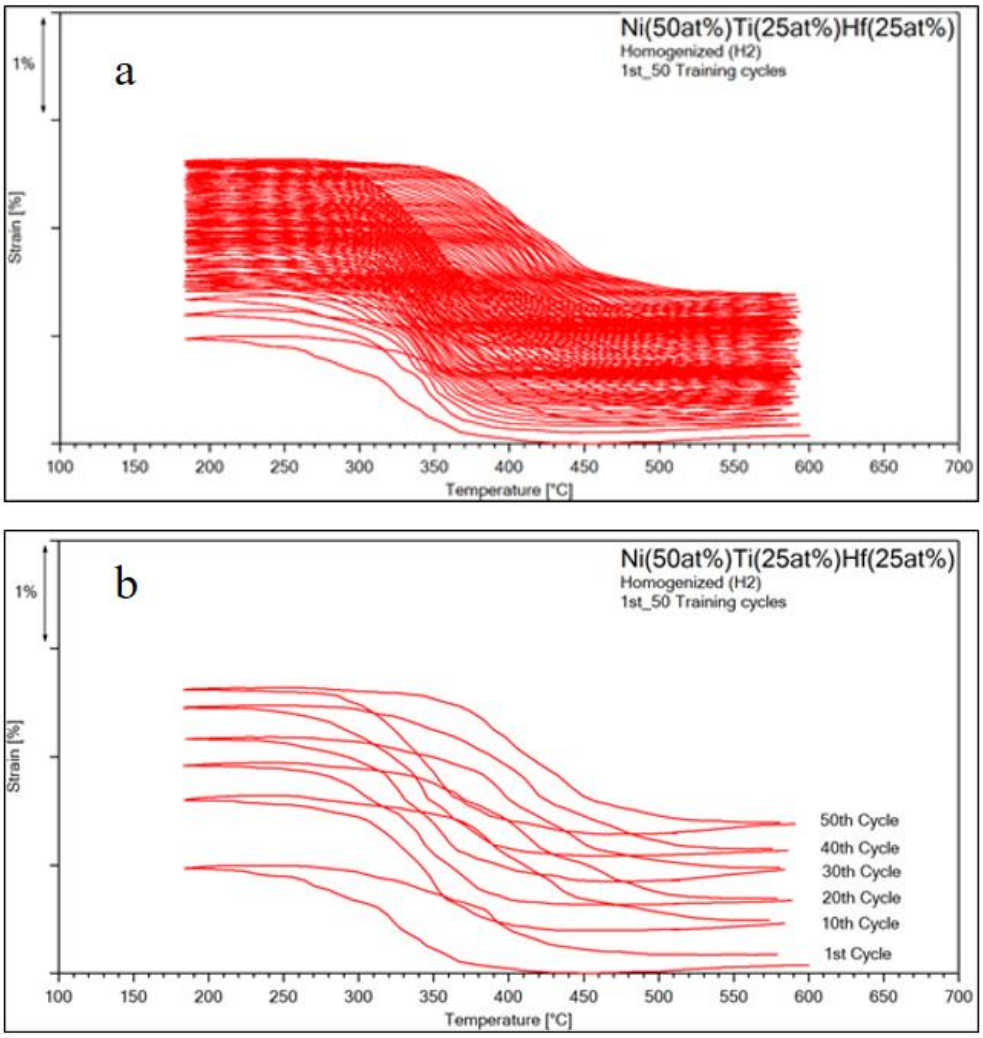

Figure 4.3-1 (a) 1st 50 Isobaric Training Cycles of the Homogenized (H2) Sample, (b) Strain vs Temperature curves obtained every ten cycles, which were selected from the 1st 50 Isobaric Training Cycles of the Homogenized (H2) Sample

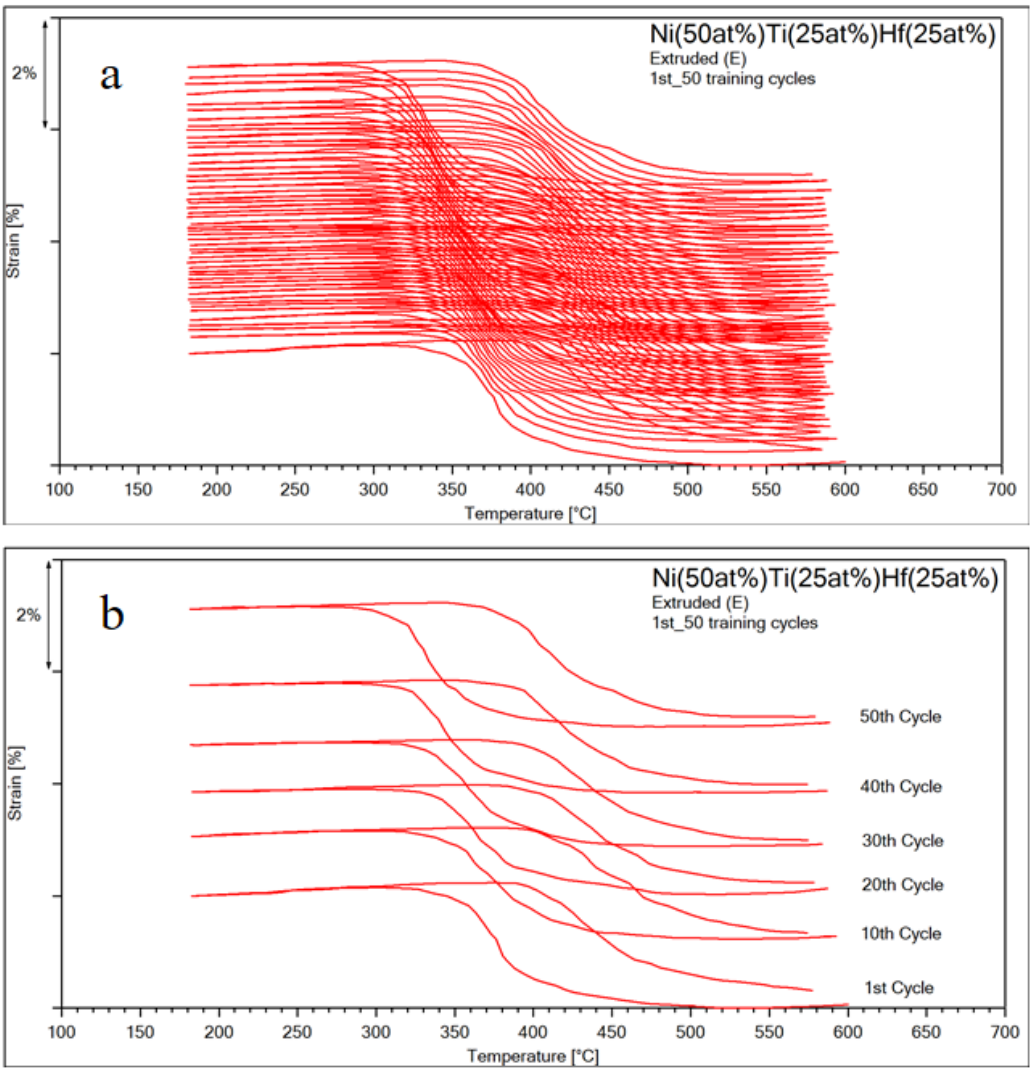

Figure 4.3-2 (a) 1st 50 Isobaric Training Cycles of the first Extruded (E) Sample, (b) Strain vs Temperature curves obtained every ten cycles, which were selected from the 1st 50 Isobaric Training Cycles of the first Extruded (E) Sample

The ε_{mar}, $\varepsilon_{aus,}$ and ε_{act} of all three samples were drawn from the strain vs temperature curves and are illustrated in Figure 4.3-4. During the 1st 50 Isobaric Training Cycles, the ε_{act} of the Extruded sample (E) was larger than that of the H2 and EE samples, and the Homogenized sample (H2) showed the lowest ε_{act} (E > EE > H2) at all. While the ε_{act} was determined as 1.8% for the first Extruded sample (E) and this percentage decreased approximately down to 1.5% for the second Extruded sample (EE) and 1% for the Homogenized sample (H2).

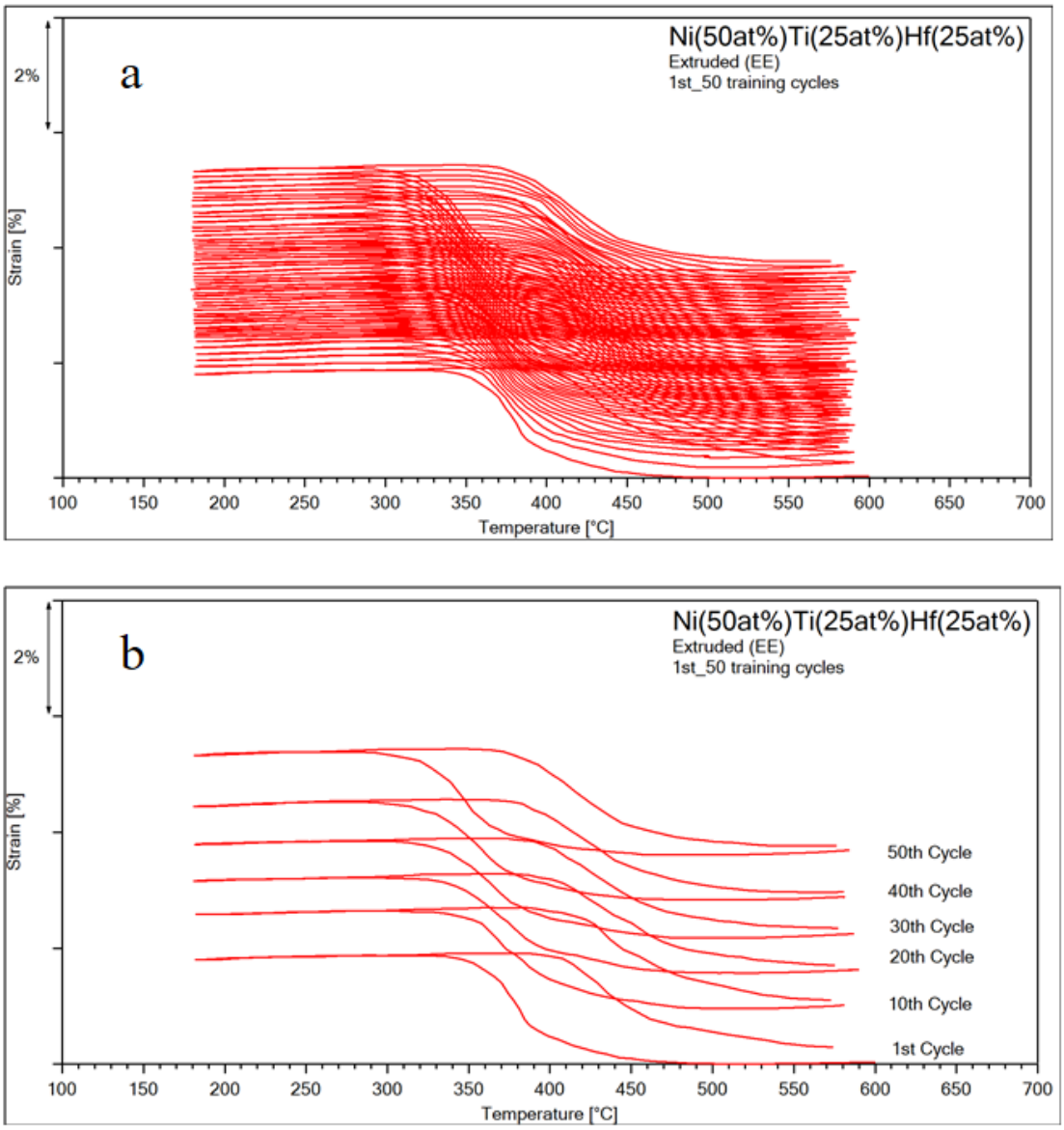

Figure 4.3-3 (a) 1st 50 Isobaric Training Cycles of the second Extruded (EE) Sample, (b) Strain vs Temperature curves obtained every ten cycles, which were selected from the 1st 50 Isobaric Training Cycles of the second Extruded (EE) Sample

In the literature, observing higher ε_{act} during isobaric training cycles may be attributed to the internal stress fields around the existing dislocation structures. Rearrangement of existing dislocations to favor the martensite-austenite transformation and the formation of desired texture with the application of the ECAE led to achieve higher ε_{act} during cycling [24]. Similarly, it can be concluded that the E and EE samples revealed higher ε_{act} than that of the H2 sample because of the internal stress fields, which favor to attain

higher transforming volume and the more favorable texture formation with extrusion. Stress fields due to the oriented dislocations and the desired texture formation might favor the martensite-austenite transformation, so the transforming volumes might be increased. Moreover, it was stated in a NiTiHf HTSMA study that the initial training cycles created oriented stress fields due to dislocation formations. After continuing training cycles, additional stress fields and dislocation formations were blocked by the stress fields, which were attained at the beginning. Therefore, new stress fields were not introduced and ε_{act} values were stabilized throughout the training [11].

Similarly, for both extruded and homogenized samples, it can be proposed that the training cycles created an internal stress field by inducing dislocations to the alloy. ε_{aus} corresponds to the accumulated ε_{irr} in the samples, which is the indication of the dislocation storage with plastic deformation and the retained martensite formation due to the pinning of martensite boundary by the generated dislocations. The ε_{aus} increment was determined to be quite higher in extruded samples that of in homogenized samples. This observation is difficult to explain right at this point since the lower increase of ε_{aus} was expected in extruded samples due to possible dislocation formations and the stress fields around them. However, there might be a possibility of inducing more favorably oriented martensite with the thermal cycles under 300MPa and this led to an increase in the ε_{aus} values.

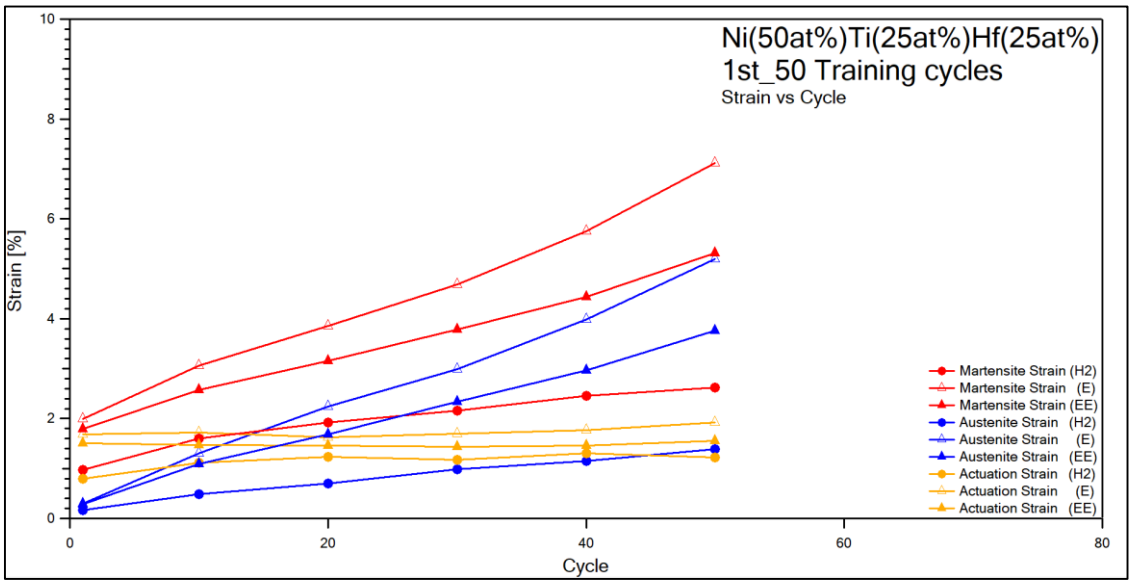

Figure 4.3-4 ε_{mar}, ε_{aus}, and ε_{act} Levels of all samples for the 1st 50 Isobaric Training Cycles

Additionally, ΔT values as the function of thermal cycles were compared in Figure 4.3-5. The ΔT values of the extruded samples were lower than that of the homogenized sample at the beginning but started to increase noticeably during the first 10 cycles and then stabilized. This is also an indication of dislocation formation with the number of training cycles in the extruded samples since ΔT is increased only when the martensite to austenite and austenite to martensite transformation becomes difficult due to the increased number of dislocations. This may be attributed to the pinning of the martensite-austenite boundary and may lead to a decrease in the mobility of this phase boundary. Therefore, more overheating and undercooling are necessary to observe phase transformations.

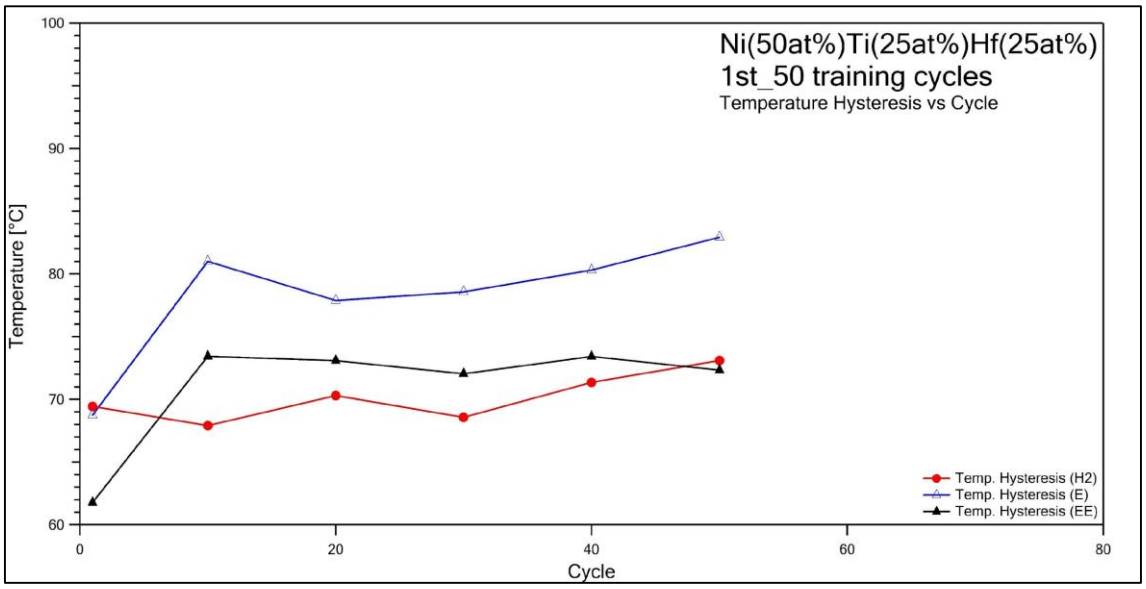

Figure 4.3-5 ΔT evolution of all samples during the 1st 50 Isobaric Training Cycles

4.4. 2nd 10 Stress-Free Thermal Cycles

As stated earlier, since experiments were conducted by heating the samples to 600°C, 100 isobaric training cycles were run as two 50 cycles to tackle the high-temperature endurance problem of black paint. Although it was not in the scope of the experimental studies at first, 2nd Stress-Free Thermal Cycles were conducted on all three test specimens after the first training to observe the initial effect of training. In Figure 4.4-1, strain vs.

temperature curves of all three specimens are plotted for the 2nd Stress-Free Thermal Cycles.

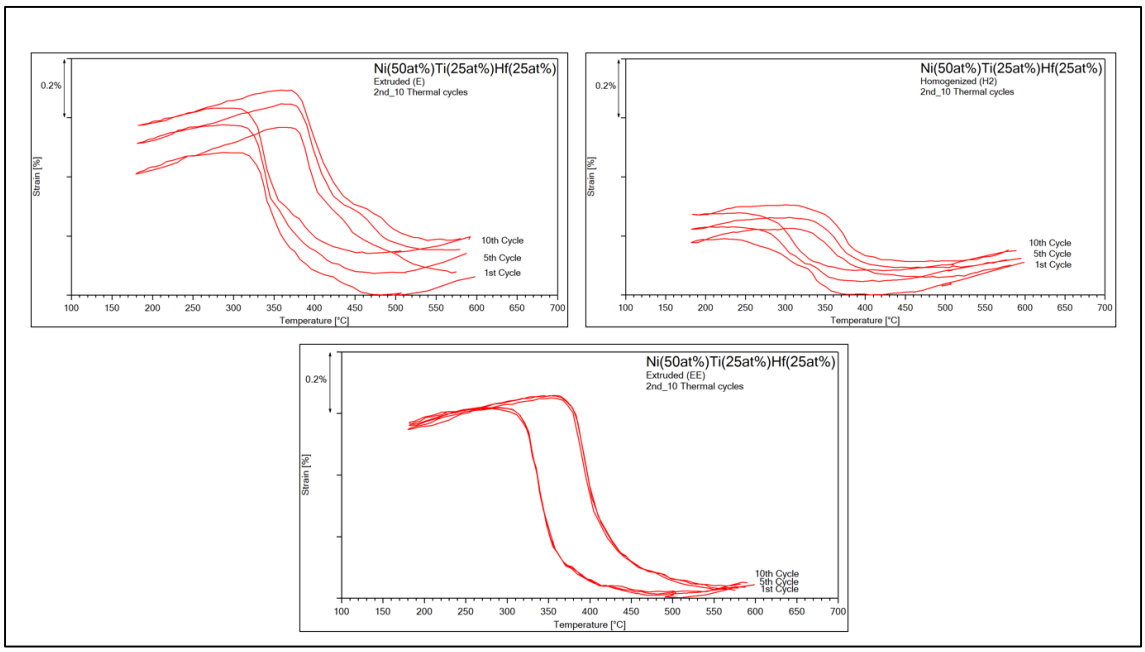

Figure 4.4-1 2nd 10 Stress-Free Thermal Cycles of All Three Samples after 1st 50 training cycles.

First of all, it is important to mention that, while the Homogenized sample (H2) did not show any TWSME during the 1st Stress-Free Thermal Cycles, a slight TWSME with 0.1% ε_{TWSM} was obtained during the 2nd Stress-Free Thermal Cycles. This could be associated with the favorable dislocation formation and the internal stress field during the first isobaric training, which led to achieving TWSME. Although a clear hysteresis was observed in the Homogenized sample (H2) after training, the ε_{TWSM} was still less than that of the first Extruded (E) and the second Extruded sample (EE). There might be two reasons behind this result, which are the formation of favorable dislocations during the extrusion process as well as during the training cycles [24] and the other one could be the texture formation with extrusion, which favors the formation of dislocation arrays to

obtain TWSME. ε_{TWSM}, ε_{mar} and ε_{aus} values were drawn from the strain vs. temperature curves of all samples in Figure 4.4-1 and are presented in Figure 4.4-2.

It should be noted that, while the first Extruded sample (E) showed higher ε_{TWSM} and ε_{act} than that of the second Extruded sample (EE) during the 1st 10 Stress-Free Thermal and the 1st 50 Isobaric Training Cycles, respectively, the EE sample yielded more ε_{TWSM} than that of the E sample during the 2nd 10 Stress-Free Thermal Cycles. To put it simply, the magnitude of the ε_{TWSM} order changed from E > EE > H2 to EE > E > H2 after the 1st 50 Isobaric Training Cycles. It seems that the second Extruded sample (EE) responded better to training and higher and more stable ε_{TWSM} values were achieved with respect to the E sample as can be seen clearly from Figure 4.4-2. While the first Extruded sample (E) exhibited approximately 0.35% of ε_{TWSM}, this value was computed at around 0.5% for the second Extruded sample (EE) during the 2nd Stress-Free Thermal Cycles.

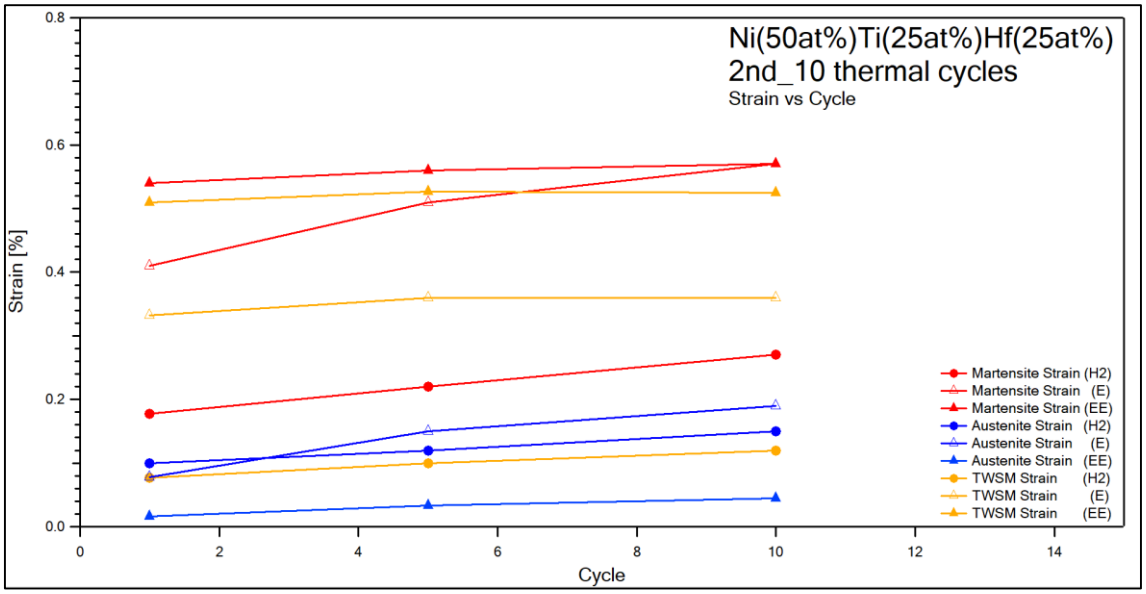

Figure 4.4-2 ε_{mar}, ε_{aus}, and ε_{act} Levels of the 2nd 10 Stress-Free Thermal Cycles

4.5. 2nd 50 Isobaric Training Cycles

As the second part of the 100 training cycles, all three samples were thermally cycled by another 50 Isobaric Training Cycles and strain vs. temperature curves are given in Figure

4.5-1. Please note that only selected cycles were drawn to clearly show the training cycles of all samples.

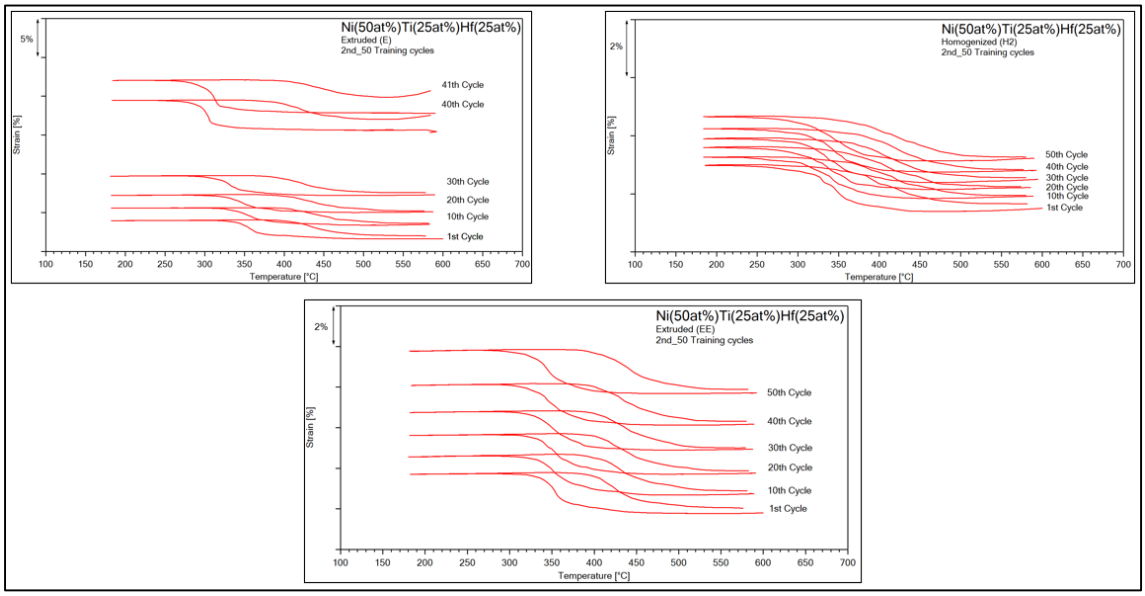

Figure 4.5-1 Strain vs Temperature Curves of 2nd 50 Isobaric Training Cycles

It is worth noting that while the Homogenized (H2) and the second Extruded (EE) sample were trained without failure with 100 cycles in total, the first Extruded (E) sample failed at the 91st training cycle. As clearly shown in Figure 4.5-2, the ε_{aus} started to increase with a higher rate than that of the increase in εmar with the 85th cycle and a notable εirr started to develop in the Extruded sample (E) as well. Therefore, the Extruded sample (E) fractured with increasing εirr under 300MPa at the 91st thermal cycle. The failure of the first extruded sample was attributed to the inappropriate coating of the sample surface with black paint. Black paint was used during all experiments to measure the surface temperature of the samples correctly. If the black paint was peeled off locally from the sample surface, the emissivity value might be changed and the temperature could not be read accurately. Therefore, the sample had risen well above the set temperature, causing premature failure.

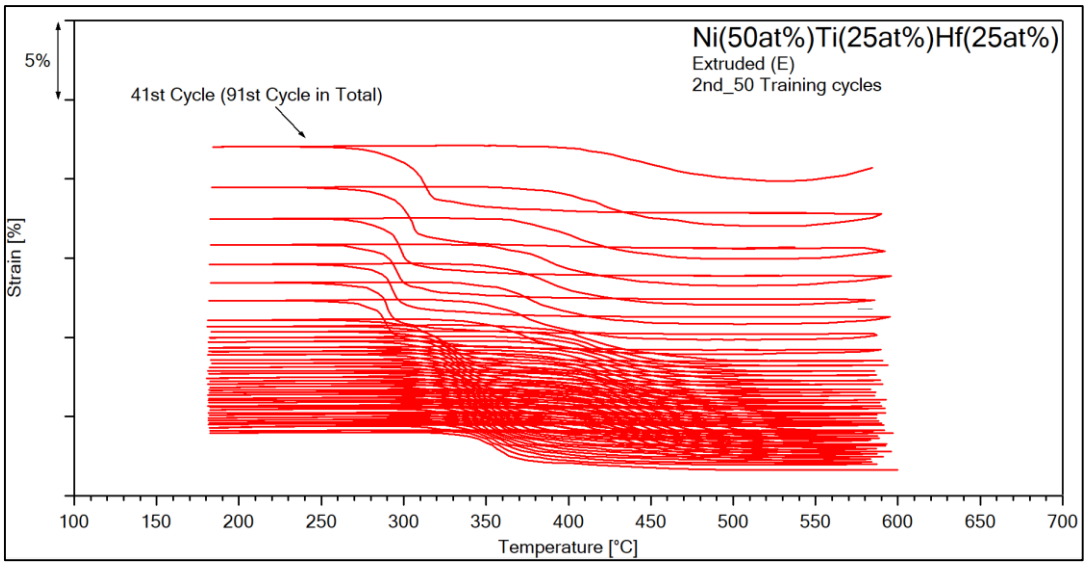

Figure 4.5-2 2nd 50 Isobaric Training Cycles of the Extruded Sample (E)

The εact values were drawn from strain vs temperature curves of 2nd 50 Isobaric Training Cycles and separately shown as a function of cycles in Figure 4.5-3. All the εact values of the samples, which were drawn from the 1st 50 training cycles and from the 2nd 50 training cycles, are presented in

Table 4.5-1 and Table 4.5-2, respectively, for comparison.

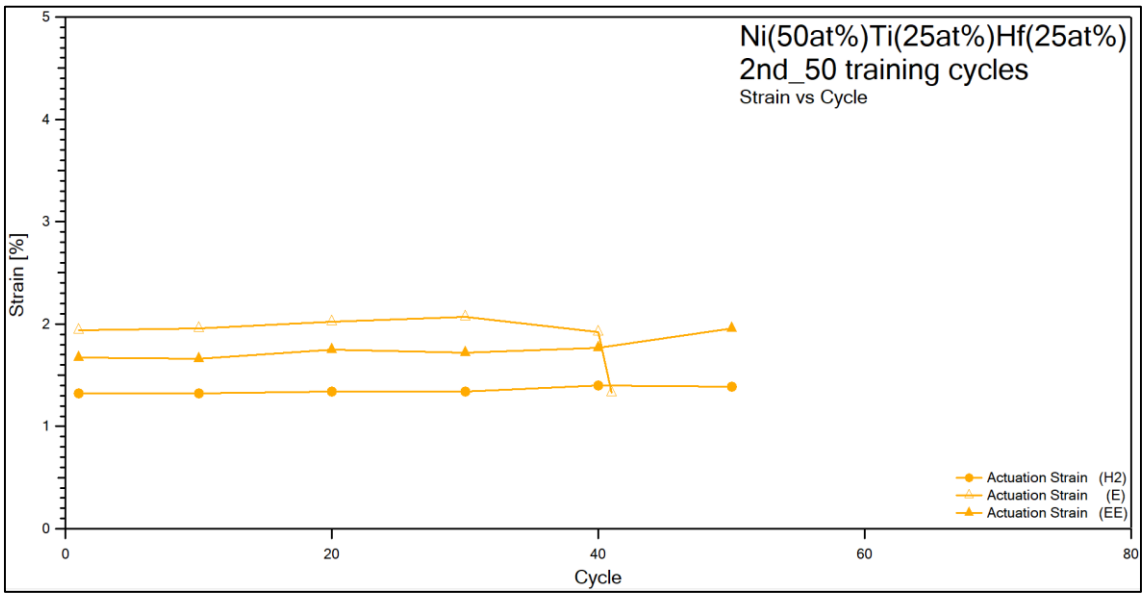

Figure 4.5-3 ε_{act} Levels of the 2nd 50 Isobaric Training Cycles

Similar to the εact results from the 1st 50 training cycles, the highest εact values were measured for the first Extruded (E) sample that was on the average of 2% until the fracture, and the lowest ε_{act} that was roughly 1.30% was attained from the Homogenized sample (H2) during the 2nd Isobaric Training Cycles. Additionally, an average of 1.75% εact value was measured from the second Extruded sample (EE). The same order of εact magnitudes was obtained (E > EE > H2) in the 2nd Isobaric Training Cycles as in the 1st Training Cycles, as can be clearly seen in

Table 4.5-1 and Table 4.5-2.

Table 4.5-1 ε_{act} of the 1st 50 Isobaric Training Cycles

		ε_{act} [%]		
	Cycle	**First Extruded (E)**	**Second Extruded (EE)**	**Homogenized (H2)**
1st 50 Isobaric Training Cycles	1	1,69	1,51	0,79
	10	1,72	1,47	1,11
	20	1,62	1,46	1,23
	30	1,7	1,44	1,18
	40	1,77	1,46	1,31
	50	1,92	1,55	1,22

Table 4.5-2 ε_{act} of the 2nd 50 Isobaric Training Cycles

		ε_{act} [%]		
	Cycle	**First Extruded (E)**	**Second Extruded (EE)**	**Homogenized (H2)**
2nd 50 Isobaric Training Cycles	1	1,94	1,67	1,32
	10	1,96	1,66	1,32
	20	2,02	1,75	1,34
	30	2,07	1,72	1,34
	40	1,92	1,77	1,4
	50	Failed	1,96	1,39

According to the values in both tables, an almost constant increment in the ε_{act} of the second Extruded (EE) and Homogenized (H2) samples was observed as well. Moreover, the ε_{act} values of all samples that were achieved in the 2nd training cycle were higher than that of the ε_{act} values obtained from the 1st training cycles. ε_{mar} and ε_{aus} values together with the ε_{act} values, which were gathered from the 2nd training cycle and are drawn in Figure 4.5-4.

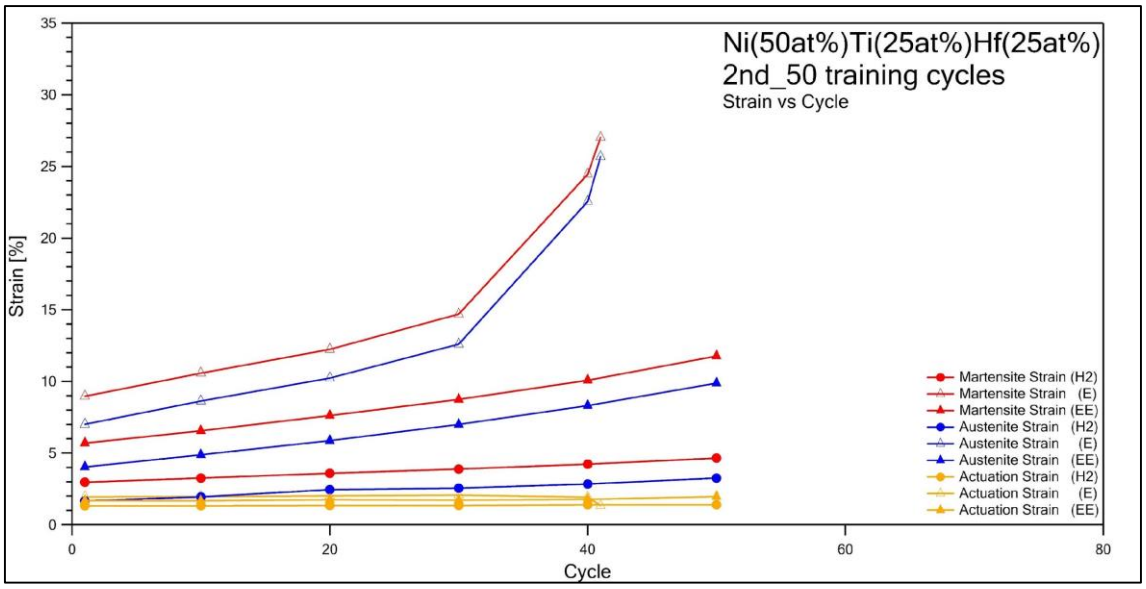

Figure 4.5-4 ε_{mar}, ε_{aus}, and ε_{act} Levels of the 2nd 50 Isobaric Training Cycles

As is clearly shown in Figure 4.5-4, the εaus values of the first extruded sample (E), which are an indication of the εirr due to plastic deformation, increased drastically with respect to the second extruded and homogenized samples. As aforementioned, the surface temperature of the first extruded sample might not be measured accurately due to the peeling of the paint from the surface. Therefore, the sample might be heated above the UCT temperature, which was set as 600°C. Then, the crack propagation together with the plastic deformation becomes very dominant and the early failure is experienced with the increase in εaus values. The drastic increase in the εaus values and the ΔT values of 1st extruded sample is actually the proof of this argument. The increase in the ΔT values of the first extruded sample is also shown in Figure 4.5-5. It is worth mentioning that the second extruded and homogenized samples showed quite stable ΔT values throughout the training cycles.

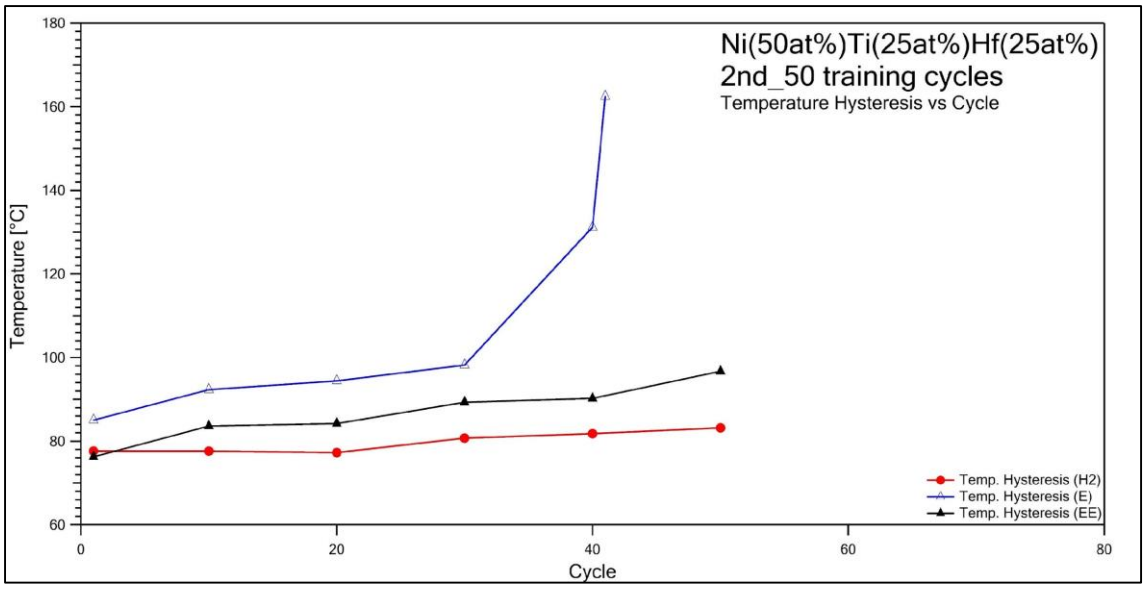

Figure 4.5-5 ΔT Values of All Samples as a function of cycles, which were gathered from the 2nd 50 Isobaric Training Cycles.

4.6. 1000 Stress-Free Two-way Shape Memory Effect (TWSME) Cycles

After completing 100 training cycles, the second Extruded (EE) and the Homogenized (H2) samples were subjected to the 1000 Stress-Free TWSME Cycles. Since the first Extruded sample (E) fractured during the training, the 1000 TWSME cycles could not be applied to this sample. Similarly, because of insufficient resistance of the black paint to high temperatures, 1000 cycles were completed at several 50-cycle steps for both specimens. The 1st 50 Stress-Free Cycles of 1000th stress-free cycles are given for the Homogenized (H2) and the Extruded sample (EE) in Figure 4.6-1.

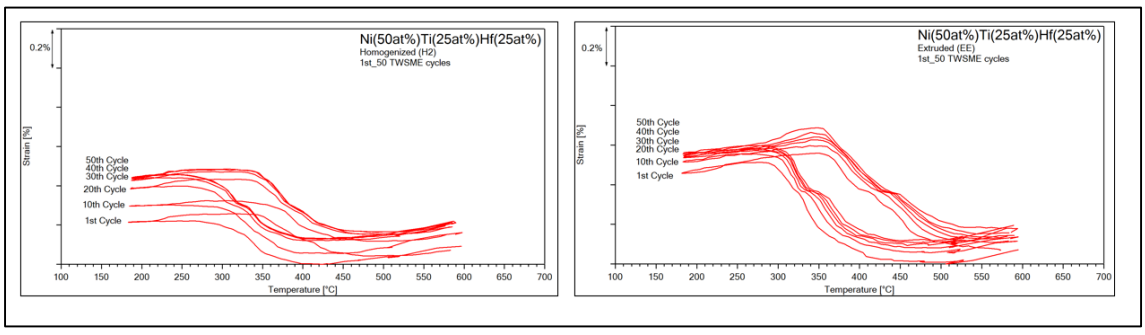

Figure 4.6-1 Strain vs. Temperature Curves of 1st 50 TWSME Cycles of 1000th TWSME cycles.

Before continuing to the remaining Stress-Free TWSME Cycles, the 2nd 10 Stress-Free Thermal Cycles, which were run after the first 50 cycle of training, and the 1st 50 TWSME Cycles were compared in terms of εTWSM to examine the effect of the 2nd 50 Isobaric Training Cycles of Homogenized Sample in Figure 4.6-2. Please keep this in mind that the 2nd 50 Isobaric Training Cycles were performed on both specimens between the 2nd 10 Stress-Free Thermal Cycles and the 1st 50 Thermal Cycles.

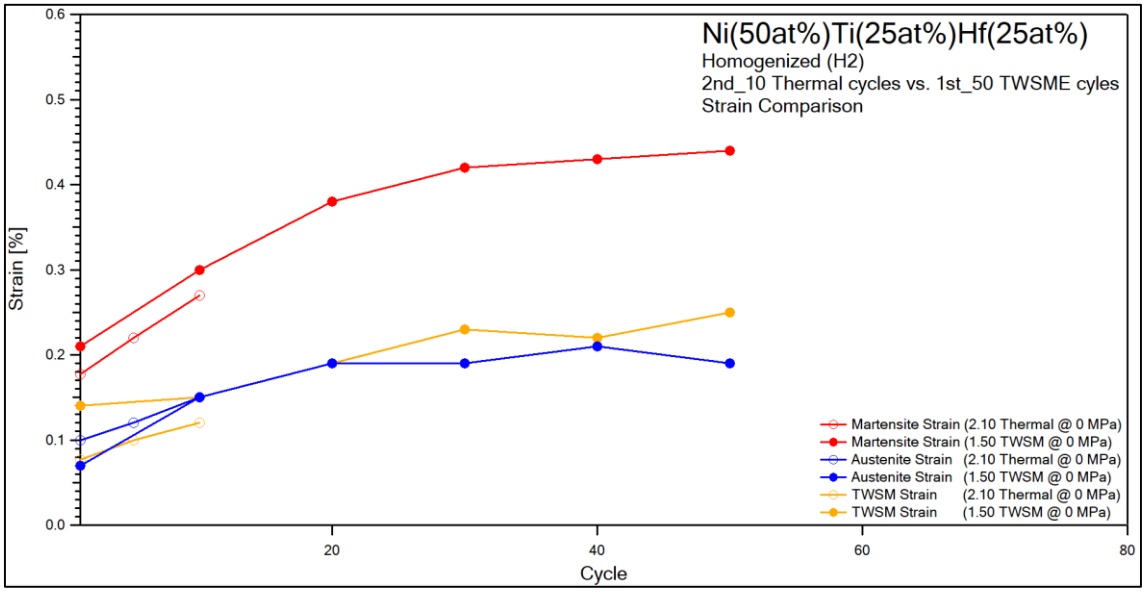

Figure 4.6-2 ε_{mar}, ε_{aus}, and ε_{TWSM} Comparison of the 2nd 10 Stress-Free Thermal Cycles and the 1st 50 Thermal Cycles of Homogenized sample-H2

While the ε_{mar}, ε_{aus}, and ε_{TWSM} comparison of the 2nd 10 Stress-Free Thermal Cycles with the 1st 50 Thermal Cycles for the Homogenized sample (H2) are depicted in Figure 4.6-2 for the same comparison for the Extruded sample (EE) can be seen in Figure 4.6-3. The ε_{TWSM} values of the H2 sample, which were obtained from the 1st 50 Stress-Free Thermal Cycles, were higher than that of the values obtained from the 2nd 10 Stress-Free Thermal Cycles. On the other hand, Extruded sample (EE) showed lower ε_{TWSM} values during the 1st 50 Stress-Free Thermal Cycles than that of the 2nd 10 Stress-Free Thermal Cycles. It is not very logical to compare the ε_{aus} values in both experiments since the number of cycles was not the same, but it may be reasonable to state that the same final values of ε_{aus} at the end of 50 stress-free thermal cycles were obtained.

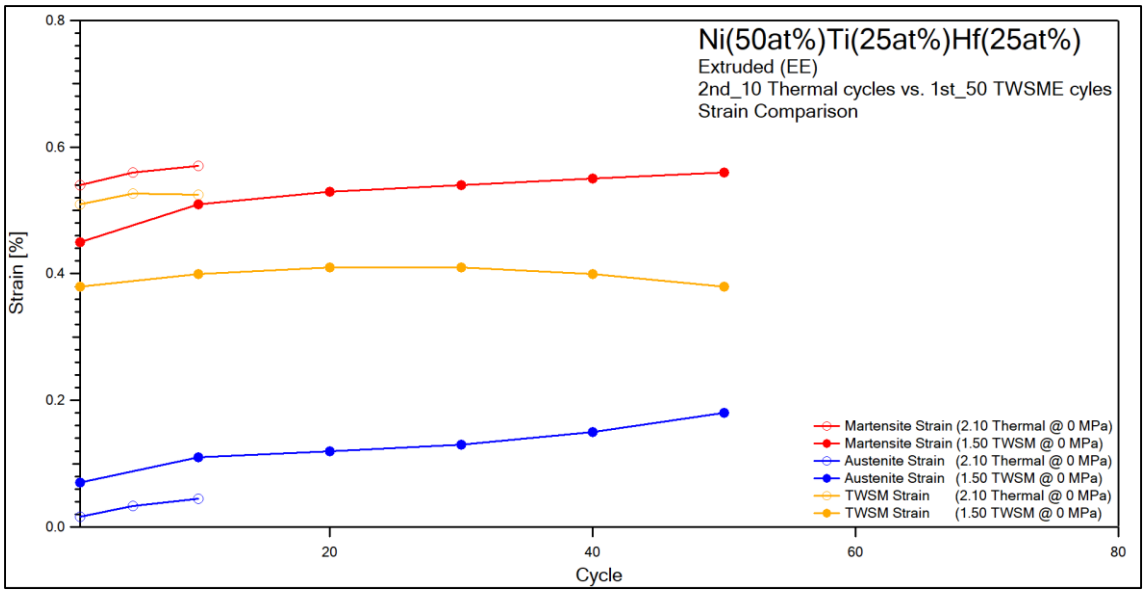

Figure 4.6-3 Martensite, Austenite, and TSWM Strain Comparison of the 2nd 10 Stress-Free Thermal Cycles and the 1st 50 Thermal Cycles (Extruded Sample-EE)

Finally, the 1000 Stress-Free TWSME Cycles were completed on both of the Homogenized (H2) and the Extruded sample (EE). The martensite, austenite, and ε_{TWSM} comparison of the two specimens are given in Figure 4.6-4. It is known that new dislocations can be thermally introduced during stress-free thermal cycles as well. Therefore, for both the Homogenized (H2) and the Extruded sample (EE), a progressive relaxation in the post-trained oriented stress fields and degradation of ε_{TWSM} due to alteration of dislocation structure were expected during the 1000 Stress-Free TWSME Cycles. However, as can be seen more detailed in Figure 4.6-5, this was not the case for the Homogenized sample (H2).

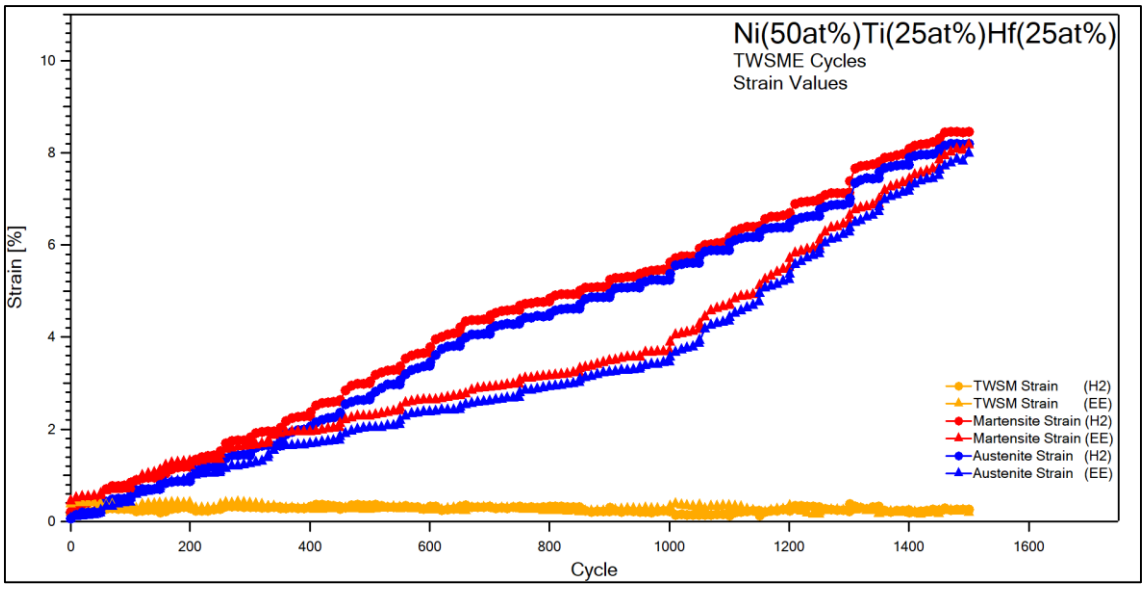

Figure 4.6-4 ε_{mar}, ε_{aus}, and ε_{TWSM} Comparison of EE and H2 Samples through 1000 Stress-Free TWSME Cycles

At first glance, the ε_{TWSM} of the Homogenized sample (H2) increased from 0.17% to 0.38% at the 500th cycle, then stabilized at 0.30% between 650th and 850th cycle during the TWSME cycles. The increasing trend in the ε_{TWSM} of Homogenized Sample (H2) at the beginning might be attributed to the thermally induced dislocation formations with the martensite-austenite phase transformation. The ε_{aus} values of the H2 sample achieved in training cycles, which were shown in Figure 4.6-4, were less than that of the EE sample. This means that less amount of dislocations was stored in the homogenized sample; therefore, homogenized sample had still less strength than that of the extruded sample, such that dislocation storage during the first 100th stress-free cycles was determined to be higher since the ε_{aus} values increased noticeably with the number of stress-free cycles as shown in Figure 4.6-4. This is also the reason in the increasing trend of ε_{TWSM} values of H2 sample as shown in Figure 4.6-5. Although a decreasing trend in the ε_{TWSM} after the 850th cycle was observed, more TWSME cycles should be performed to monitor the degradation of TWSME due to dislocation annihilation with the thermal cycles.

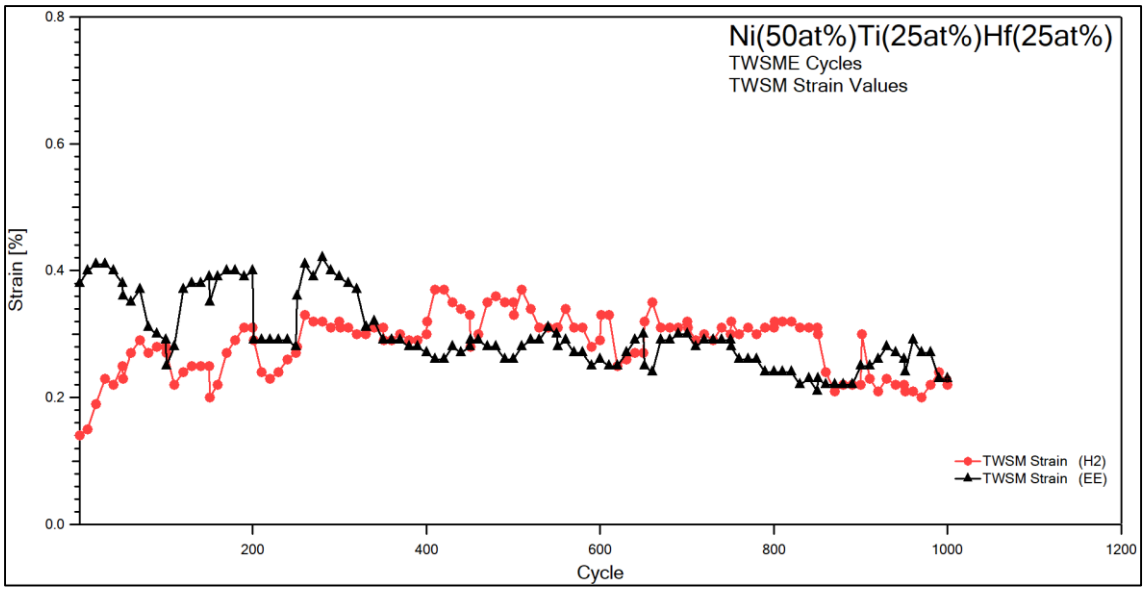

Figure 4.6-5 The ε_{TWSM} Comparison of the Extruded Sample (EE) through 1000 Stress-Free TWSME Cycles

On the other hand, the ε_{TWSM} of the Extruded sample (EE) dropped from 0.40% to 0.30% at the 350th cycle, then stabilized at around 0.25% during the TWSME cycles. As expected, the annihilation of the training-induced oriented dislocations and the relaxation of the stress fields around these dislocations were experienced due to the very high upper cycle temperature (600°C) by the extruded sample and thus ε_{TWSM} was reduced with the number of stress-free thermal cycles. When looking at the 200 thermal cycles in Figure 4.6-5, the same magnitude of ε_{TWSM} was observed in both samples.

5. CONCLUSION

In this study, the following main conclusions can be drawn from the results of the experiments. The first objective of the present study was observing the effect of homogenization on the TWSME of hot extruded Ni50Ti25Hf25 (at%) HTSMA. First of all, it is worth mentioning that achieving TWSME in HTSMAs is very difficult since the temperature up to which the samples are heated is very high. This temperature is called as UCT, which is set to obtain full austenitic transformation. It was previously shown in the literature that, TWSME was not attained in TiNiPt HTSMA [10]. While the Extruded Samples (E and EE) revealed TWSME, the homogenized (H2) sample did not show an apparent ε_{TWSM} during the 1st 10 Stress-Free Thermal Cycle before the training cycles. Therefore, it can be concluded that homogenization deteriorates the TWSME because of the annihilation of extrusion-induced favorably oriented dislocations and internal stress fields, which are necessary formations to obtain certain martensite plates/variants during cooling under no-load condition.

The other intention of this study was achieving the TWSME in Ni50Ti25Hf25 (at%) by shape memory/isobaric training (i.e., training under constant load) and observing the stability of this effect for long stress-free thermal cycles. The ε_{act} of both Extruded samples (E and EE) were more than that of the Homogenized sample (H2) during the 100 training cycles and this can be attributed to the support of extrusion-induced favorably oriented dislocations and the internal stress fields around them to the martensite-austenite phase transformation. Additionally, texture formation with extrusion might be the reason of attaining higher ε_{act} values in training cycles. Moreover, a stable increase in the actuation strain was observed in all Ni50Ti25Hf25 (at%) samples, possibly due to favorably oriented dislocation formation through tensile direction during the training process. Since a very consistent ε_{act} and ΔT values were gathered from all specimens during 100 training cycles under 300 MPa, it was concluded that 100 training cycle was sufficient to obtain a stable TWSME response in Ni50Ti25Hf25 (at%) alloy.

During the thermo-mechanical training, while the second Extruded sample (EE) was able to complete the entire 100 training cycles under 300 MPa, the first Extruded sample (E) failed at the 91st cycle. However, it was regarded as reasonable because the reaction of

different extruded samples cut from the same billet may show different shape memory behaviors due to the extrusion-induced microstructural nonuniformity. Besides, the black paint, which was used to coat the surface of the samples to accurately measure and control the sample temperatures, might be peeled off, thus the temperature was not able to be measured and controlled. The sample was probably heated to a temperature that was higher than the set UCT. If this was the case, then the crack propagation and plastic deformation rates became higher and the early failure was experienced. The difference between the first Extruded (E) and the second Extruded (EE) sample was also determined during training cycles. While the ε_{act} values of the first Extruded (E) sample were higher during the 1st 50 Isobaric cycles, the second Extruded (EE) sample showed higher ε_{act} values than that of the first Extruded (E) sample during the 2nd 50 training cycles. This alteration can also be attributed to the different reactions of the sample to training due to the microstructural nonuniformity induced by extrusion.

Finally, observing the TWSME of Ni50Ti25Hf25 (at%) for long thermal cycles was the last purpose of the present study. While the Extruded sample (EE) showed more ε_{TWSM} values at the beginning of 1000 TWSME cycles, possibly due to extrusion-induced favorably oriented dislocations and the internal stress fields. However, ε_{TWSM} values of the Homogenized sample (H2) increased and reached to the ε_{TWSM} values obtained from Extruded sample (EE). ε_{TWSM} of both samples became almost equal at around the 800th TWSME cycle. ε_{TWSM} of Extruded Sample decreased with the number of stress-free thermal cycles due to the annihilation of favorably oriented dislocations and due to the relaxation of the stress field around these dislocations at high temperatures. On the other hand, ε_{TWSM} of the homogenized sample increased at the beginning, which can be attributed to the formation of thermally induced dislocation with the thermal cycles, which enhanced the TWSME. However, it should be noted that the ε_{TWSM} of Ni50Ti25Hf25 (at%) HTSMA was found to be way less than that of TWMS strain values that were previously reported in the NiTiHf studies in the literature. On the other hand, NiTiHf alloys, which were previously studied in the literature, have lower TTs than that of the one that was used in this study. Thus, Ni50Ti25Hf25 (at%) HTSMA alloy had to be heated to higher UCT such that dislocation annihilation became more dominant. Therefore, it can be suggested that Ni50Ti25Hf25 (at%) HTSMAs can be trained more

than 300 MPa constant stress to induce more favorably oriented dislocations to enhance the TWSME.

6. REFERENCES

[1] H. H. Saygili, “THE DEVELOPMENT OF A FATIGUE TEST MACHINE TO INVESTIGATE THE FUNCTIONAL FATIGUE LIFE OF HIGH TEMPERATURE SHAPE MEMORY ALLOYS AND THE DETERMINATION OF THE FUNCTIONAL FATIGUE LIFE OF THESE ALLOYS,” M.Sc. Thesis, Graduate School of Science and Engineering of Hacettepe University, Ankara, 2018.

[2] J. Ma, I. Karaman, and R. D. Noebe, “High temperature shape memory alloys,” *http://dx.doi.org/10.1179/095066010X12646898728363*, vol. 55, no. 5, pp. 257–315, Sep. 2013, doi: 10.1179/095066010X12646898728363.

[3] H. E. Karaca, E. Acar, H. Tobe, and S. M. Saghaian, “NiTiHf-based shape memory alloys,” *https://doi.org/10.1179/1743284714Y.0000000598*, vol. 30, no. 13, pp. 1530–1544, Nov. 2014, doi: 10.1179/1743284714Y.0000000598.

[4] K. Otsuka and X. Ren, “Physical metallurgy of Ti–Ni-based shape memory alloys,” *Progress in Materials Science*, vol. 50, no. 5, pp. 511–678, Jul. 2005, doi: 10.1016/J.PMATSCI.2004.10.001.

[5] S. M. Saghaian, H. E. Karaca, H. Tobe, M. Souri, R. Noebe, and Y. I. Chumlyakov, “Effects of aging on the shape memory behavior of Ni-rich Ni50.3Ti29.7Hf20 single crystals,” *Acta Materialia*, vol. 87, pp. 128–141, Apr. 2015, doi: 10.1016/J.ACTAMAT.2014.12.040.

[6] K. Otsuka and X. Ren, “Recent developments in the research of shape memory alloys,” *Intermetallics (Barking)*, vol. 7, no. 5, pp. 511–528, May 1999, doi: 10.1016/S0966-9795(98)00070-3.

[7] A. Concilio, V. Antonucci, F. Auricchio, L. Lecce, and E. Sacco, *Shape memory alloy engineering : for aerospace, structural and biomedical applications.*, 2nd Edition. Elsevier.

[8] O. Akgul, H. O. Tugrul, and B. Kockar, “Effect of the cooling rate on the thermal and thermomechanical behavior of NiTiHf high-temperature shape memory alloy,” *Journal of Materials Research*, vol. 35, no. 12, pp. 1572–1581, Jun. 2020, doi: 10.1557/JMR.2020.139.

[9] H. H. Saygili, H. O. Tugrul, and B. Kockar, “Effect of Aging Heat Treatment on the High Cycle Fatigue Life of Ni50.3Ti29.7Hf20 High-Temperature Shape Memory Alloy,” *Shape Memory and Superelasticity 2018 5:1*, vol. 5, no. 1, pp. 32–41, Dec. 2018, doi: 10.1007/S40830-018-00202-5.

[10] K. C. Atli, I. Karaman, R. D. Noebe, and D. Gaydosh, “The effect of training on two-way shape memory effect of binary NiTi and NiTi based ternary high temperature shape memory alloys,” *Materials Science and Engineering: A*, vol. 560, pp. 653–666, Jan. 2013, doi: 10.1016/J.MSEA.2012.10.009.

[11] X. L. Meng, Y. F. Zheng, W. Cai, and L. C. Zhao, “Two-way shape memory effect of a TiNiHf high temperature shape memory alloy,” *Journal of Alloys and Compounds*, vol. 372, no. 1–2, pp. 180–186, Jun. 2004, doi: 10.1016/j.jallcom.2003.10.020.

[12] Z. Eleonora, “One Way and Two Way-Shape Memory Effect: Thermo-Mechanical Characterization of Ni-Ti wires,” M.Sc. Thesis, Universita degli Studi di Pavia, Pavia, 2008.

[13] M. Nishida and T. Honma, “All-round shape memory effect in Ni-rich TiNi alloys generated by constrained aging,” *Scripta Metallurgica*, vol. 18, no. 11, pp. 1293–1298, 1984, doi: 10.1016/0036-9748(84)90125-X.

[14] C. Hayrettin, O. Karakoc, I. Karaman, J. H. Mabe, R. Santamarta, and J. Pons, “Two way shape memory effect in NiTiHf high temperature shape memory alloy tubes,” *Acta Materialia*, vol. 163, pp. 1–13, Jan. 2019, doi: 10.1016/J.ACTAMAT.2018.09.058.

[15] O. Karakoc *et al.*, “Effects of training on the thermomechanical behavior of NiTiHf and NiTiZr high temperature shape memory alloys,” *Materials Science and Engineering: A*, vol. 794, p. 139857, Sep. 2020, doi: 10.1016/J.MSEA.2020.139857.

[16] J. Mohd Jani, M. Leary, A. Subic, and M. A. Gibson, “A review of shape memory alloy research, applications and opportunities,” *Materials and Design*, vol. 56, pp. 1078–1113, Apr. 2014, doi: 10.1016/J.MATDES.2013.11.084.

[17] S. Hirose, K. Ikuta, and Y. Umetani, “Development of shape-memory alloy actuators. Performance assessment and introduction of a new composing

approach," *Advanced Robotics*, vol. 3, no. 1, pp. 3–16, 1989, doi: 10.1163/156855389X00145.

[18] A. Nespoli, S. Besseghini, S. Pittaccio, E. Villa, and S. Viscuso, "The high potential of shape memory alloys in developing miniature mechanical devices: A review on shape memory alloy mini-actuators," *Sensors and Actuators, A: Physical*, vol. 158, no. 1, pp. 149–160, Mar. 2010, doi: 10.1016/J.SNA.2009.12.020.

[19] R. Velázquez, E. Pissaloux, J. Szewczyk, and M. Hafez, "Miniature shape memory alloy actuator for tactile binary information display," *Proceedings - IEEE International Conference on Robotics and Automation*, vol. 2005, pp. 1344–1349, 2005, doi: 10.1109/ROBOT.2005.1570302.

[20] G. S. Bigelow, S. A. Padula, A. Garg, D. Gaydosh, and R. D. Noebe, "Characterization of ternary NiTiPd high-temperature shape-memory alloys under load-biased thermal cycling," *Metallurgical and Materials Transactions A: Physical Metallurgy and Materials Science*, vol. 41, no. 12, pp. 3065–3079, Dec. 2010, doi: 10.1007/S11661-010-0365-5/FIGURES/16.

[21] K. C. Atli, I. Karaman, R. D. Noebe, G. Bigelow, and D. Gaydosh, "Work production using the two-way shape memory effect in NiTi and a Ni-rich NiTiHf high-temperature shape memory alloy," *Smart Materials and Structures*, vol. 24, no. 12, p. 125023, Nov. 2015, doi: 10.1088/0964-1726/24/12/125023.

[22] S. Padula, G. Bigelow, R. Noebe, D. Gaydosh, and A. Garg, "Challenges and Progress in the Development of High-Temperature Shape Memory Alloys Based on NiTiX Compositions for High-Force Actuator Applications".

[23] K. C. Atli, I. Karaman, and R. D. Noebe, "Work output of the two-way shape memory effect in Ti50.5Ni 24.5Pd25 high-temperature shape memory alloy," *Scripta Materialia*, vol. 65, no. 10, pp. 903–906, Nov. 2011, doi: 10.1016/J.SCRIPTAMAT.2011.08.006.

[24] B. Kockar, I. Karaman, J. I. Kim, and Y. Chumlyakov, "A method to enhance cyclic reversibility of NiTiHf high temperature shape memory alloys," *Scripta Materialia*, vol. 54, no. 12, pp. 2203–2208, Jun. 2006, doi: 10.1016/J.SCRIPTAMAT.2006.02.029.

[25] J. Cui *et al.*, “Combinatorial search of thermoelastic shape-memory alloys with extremely small hysteresis width,” *Nature Materials 2006 5:4*, vol. 5, no. 4, pp. 286–290, Mar. 2006, doi: 10.1038/nmat1593.

[26] O. Benafan and D. J. Gaydosh, “High temperature shape memory alloy Ni50.3Ti29.7Hf20 torque tube actuators,” *Smart Materials and Structures*, vol. 26, no. 9, Aug. 2017, doi: 10.1088/1361-665X/AA7EF4.

[27] E. Acar, M. Çalışkan, and H. E. Karaca, “Differential scanning calorimetry response of aged NiTiHfPd shape memory alloys,” *Applied Physics A: Materials Science and Processing*, vol. 125, no. 4, Apr. 2019, doi: 10.1007/S00339-019-2543-7.

[28] G. Airoldi, G. Riva, B. Rivolta, and M. Vanelli, “DSC calibration in the study of shape memory alloys,” *Journal of Thermal Analysis*, vol. 42, no. 4, pp. 781–791, Oct. 1994, doi: 10.1007/BF02546750.

[29] E. Akin, O. Akgul, H. O. Tugrul, G. Dugan, and B. Kockar, “Investigating the effect of hot extrusion and annealing to the functional fatigue behavior of Ni50Ti30Hf20 high temperature shape memory alloy,” *Smart Materials and Structures*, vol. 30, no. 10, p. 105017, Aug. 2021, doi: 10.1088/1361-665X/AC1BEE.

[30] O. Akgul, “INVESTIGATING THE EFFECT OF LOW HEATING-COOLING RATE AND THE THERMOMECHANICAL TREATMENTS ON THE SHAPE MEMORY BEHAVIOR OF NITIHF ALLOYS,” M.Sc. Thesis, Graduate School of Science and Engineering of Hacettepe University, Ankara, 2022.